FORMATION OF MONOLAYERS BY THE COADSORPTION OF THIOLS ON GOLD: VARIATION IN THE LENGTH OF THE HEAD GROUP, TAIL GROUP, AND SOLVENT

C. D. Bain, J. Evall, and G. M. Whitesides*
Department of Chemistry
Harvard University
Cambridge MA 02138

Technical Report No. 19 (May 1989)

Interim Technical Report

(Accepted for publication in J. Am. Chem. Soc.)

PREPARED FOR DEFENSE ADVANCED RESEARCH PROJECTS AGENCY
1400 Wilson Boulevard
Arlington VA 22209

DEPARTMENT OF THE NAVY
Office of Naval Research, Code 1130P
800 North Quincy Street
Arlington VA 22217-5000

ARPA Order No.: NR 356-856
Contract No.: N00014-85-K-0898
Effective Date: 85 September 01
Expiration Date: 89 May 31

Principal Investigator: George M. Whitesides
(617) 495-9430

The views and conclusions in this document are those of the authors and should not be interpreted as necessarily representing the official policies, either expressed or implied, of the Defense Advanced Research Projects Agency or the U.S. Government.

SECURITY CLASSIFICATION OF THIS PAGE

REPORT DOCUMENTATION PAGE

1a. REPORT SECURITY CLASSIFICATION Unclassified	1b. RESTRICTIVE MARKINGS
2a. SECURITY CLASSIFICATION AUTHORITY	3. DISTRIBUTION / AVAILABILITY OF REPORT Approved for public release; distribution unlimited
2b. DECLASSIFICATION / DOWNGRADING SCHEDULE	
4. PERFORMING ORGANIZATION REPORT NUMBER(S) Technical Report # 19	5. MONITORING ORGANIZATION REPORT NUMBER(S)
6a. NAME OF PERFORMING ORGANIZATION Harvard University 6b. OFFICE SYMBOL (*If applicable*)	7a. NAME OF MONITORING ORGANIZATION Office of Naval Research
6c. ADDRESS (*City, State, and ZIP Code*) Office of Sponsored Research Holyoke Center, Fourth Floor Cambridge MA 02138-4993	7b. ADDRESS (*City, State, and ZIP Code*) Code 1130P 800 North Quincy Street Arlington VA 22217-5000
8a. NAME OF FUNDING / SPONSORING ORGANIZATION ONR/DARPA 8b. OFFICE SYMBOL (*If applicable*)	9. PROCUREMENT INSTRUMENT IDENTIFICATION NUMBER
8c. ADDRESS (*City, State, and ZIP Code*) 800 North Quincy Street Arlington VA 22217-5000	10. SOURCE OF FUNDING NUMBERS PROGRAM ELEMENT NO. 85-K-0898 / PROJECT NO. NR 356-856 / TASK NO / WORK UNIT ACCESSION NO

11. TITLE (*Include Security Classification*)
"Formation of Monolayers by the Coadsorption of Thiols on Gold: Variation in the Head Group, Tail Group, and Solvent"

12. PERSONAL AUTHOR(S)
Colin D. Bain, J. Evall, G. M. Whitesides

13a. TYPE OF REPORT	13b. TIME COVERED	14. DATE OF REPORT (*Year, Month, Day*)	15. PAGE COUNT
Interim	FROM _____ TO _____	May 1989	

16. SUPPLEMENTARY NOTATION

17. COSATI CODES			18. SUBJECT TERMS (*Continue on reverse if necessary and identify by block number*)
FIELD	GROUP	SUB-GROUP	self-assembly, monolayers, thols, gold, coadsorption

19. ABSTRACT (*Continue on reverse if necessary and identify by block number*)

Long-chain alkanethiols, $HS(CH_2)_nX$, adsorb from solution onto gold and form oriented, ordered monolayers. Although alkyl chains terminated by other functional groups (e.g., trialkylphosphines, dialkyl disulfides and dialkyl sulfides) also form monolayers on gold that are stable at room temperature, thiols are adsorbed preferentially from solutions containing mixtures of a thiol and one of these other adsorbates. Surfaces containing more than one functional group can be generated by coadsorption of two or more thiols from solution. In general, the ratio of the concentrations of the two components in a mixed monolayer is not the same as in solution but reflects the relative solubilities of the components in solution and interactions between the tail groups, X, in the monolayer. Multi-component monolayers do not phase-segregate into single-component domains large enough to influence the contact angle (a

20. DISTRIBUTION / AVAILABILITY OF ABSTRACT	21. ABSTRACT SECURITY CLASSIFICATION	
☒ UNCLASSIFIED/UNLIMITED ☐ SAME AS RPT ☐ DTIC USERS		
22a. NAME OF RESPONSIBLE INDIVIDUAL Dr. Joanne Milliken	22b. TELEPHONE (*Include Area Code*)	22c. OFFICE SYMBOL

DD FORM 1473, 84 MAR — 83 APR edition may be used until exhausted. All other editions are obsolete.

SECURITY CLASSIFICATION OF THIS PAGE

19. ABSTRACT (Cont'd)

few tens of angstroms across), but also do not act as ideal two-dimensional solutions. In the two-component systems $HS(CH_2)_nX/HS(CH_2)_nCH_3$ in ethanol, where X is a polar tail group such as $-CH_2OH$ or -CN, adsorption of the polar component is particularly disfavored at low concentrations of the polar component in the monolayer. These isotherms may arise from poor solvation of the polar tail groups in the quasi-two-dimensional alkane solution provided by the methyl tail groups. From dilute solutions in alkanes, adsorption of $HS(CH_2)_{10}CH_2OH$ is strongly preferred over $HS(CH_2)_{10}CH_3$, probably due to the stabilization afforded by intramonolayer hydrogen bonds between the hydroxyl tail groups. The wettability of mixed monolayers is not linear in the composition of the surface. In a surface comprising a polar and a nonpolar component, the polar component is more hydrophilic when its concentration in the monolayer is low than when the monolayer is composed largely of the polar component.

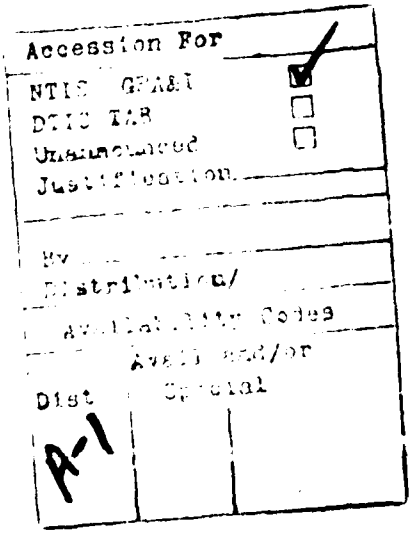

Submitted to J AM CHEM SOC

Formation of Monolayers by the Coadsorption of Thiols on Gold: Variation in the Head Group, Tail Group, and Solvent[1]

Colin D. Bain[2], Joe Evall and George M. Whitesides*

Department of Chemistry,

Harvard University,

Cambridge, Massachusetts 02138

Abstract.

Long-chain alkanethiols, $HS(CH_2)_nX$, adsorb from solution onto gold and form oriented, ordered monolayers. Although alkyl chains terminated by other functional groups (e.g. trialkylphosphines, dialkyl disulfides and dialkyl sulfides) also form monolayers on gold that are stable at room temperature, thiols are adsorbed preferentially from solutions containing mixtures of a thiol and one of these other adsorbates. Surfaces containing more than one functional group can be generated by coadsorption of two or more thiols from solution. In general, the ratio of the concentrations of the two components in a mixed monolayer is not the same as in solution but reflects the relative solubilities of the components in solution and interactions between the tail groups, X, in the monolayer. Multi-component monolayers do not phase-segregate into single-component domains large enough to influence the contact angle (a few tens of angstroms across), but also do not act as ideal two-dimensional solutions. In the two-component system $HS(CH_2)_nX/HS(CH_2)_nCH_3$ in ethanol, where X is a polar tail group such as $-CH_2OH$ or -CN, adsorption of the polar component is particularly disfavored at low concentrations of the polar component in the monolayer. These isotherms may arise from poor solvation of the polar tail groups in the quasi-two dimensional alkane solution provided by the methyl tail groups. From dilute solutions in alkanes, adsorption of $HS(CH_2)_{10}CH_2OH$ is strongly preferred over $HS(CH_2)_{10}CH_3$, probably due to the stabilization afforded by intramonolayer hydrogen bonds between the hydroxyl tail groups. The wettability of mixed monolayers is not linear in the composition of the surface. In a surface comprising a polar and a nonpolar component, the polar component is more hydrophilic when its concentration in the monolayer is low than when the monolayer is composed largely of the polar component.

Introduction.

The formation of oriented monolayer films on a surface by the spontaneous adsorption of molecules from solution is known as self-assembly.[3] Two systems of self-assembled monolayers have shown great promise as a means of controlling the chemical structure of organic surfaces: alkyl trichlorosilanes on silicon[4] and organosulfur compounds on noble metals such as gold[5,6,7] and silver.[8] In a previous paper[9] we have studied the formation, characterization and properties of monolayers formed by the adsorption of *n*-alkanethiols, $HS(CH_2)_nX$, on gold. In these monolayers the chemistry, structure and properties of the surface were controlled by varying the tail group, X.[10] The range of properties that can be obtained in homogeneous monolayers of a single thiol is, however, limited. Greater control over the structure of the monolayer is afforded by coadsorption of two or more thiols that differ in the nature of the tail group[11] or the length of the hydrocarbon chain.[12] This paper is the first of two that examine monolayers formed by the coadsorption of two species that differ in the chain length, the tail group, or the nature of the head group that binds the components of the monolayer to the gold surface. Our aims in this work are to understand how the composition of the monolayer is related to the concentrations of the adsorbates in solution, to elucidate the structure of monolayers containing two components, and to study the properties of surfaces containing more than one functional group.

First, we present a brief survey of organic functional groups, other than thiols, that coordinate to gold and form stable monolayers. Second, we examine monolayers formed from thiols with the same chain length but with different tail groups. Third, we address the effect of solvent on the composition of the monolayers, and its implications for the mechanism of adsorption. In the companion paper we discuss mixed monolayers in which the two components have different chain lengths.[13]

The general strategy in these studies was to prepare a series of dilute solutions containing two components, $A(CH_2)_nX$ and $B(CH_2)_mY$, in a range of mole fractions but with the same total concentration of adsorbate. The head group (A, B), the tail group (X, Y), the chain length, or a combination of these three, differed between the two adsorbates. Gold slides were immersed in these solutions and monolayers allowed to form under ambient conditions of temperature and pressure. In the text, we designate monolayers adsorbed from pairs of thiols as X/Y to indicate the pair of tail groups that are exposed at the surface of the monolayers. Thus, for example, the monolayer prepared by adsorption of thiols from a solution containing $HS(CH_2)_{10}CH_2OH$ and $HS(CH_2)_{10}CH_3$ would be designated OH/Me. We determined the composition of the monolayers as a function of the concentrations in solution by X-ray photoelectron spectroscopy (XPS), ellipsometry, or contact angle. XPS proved to be a versatile, quantitative tool for analyzing monolayers containing more than one component. If either of the head groups or either of the tail groups contained a unique heteroatom, the composition of the monolayers could be determined directly from the relative intensities of the photoelectron signals from the heteroatom. If the two components differed in chain length, the attenuation of the photoelectrons from the gold substrate by the overlaying monolayer provided an indirect measure of the thickness of the monolayer and hence of its composition. Optical ellipsometry provided an independent determination of the thickness of the monolayer. To utilize contact angles as an indicator of the composition of the monolayer, we chose pairs of adsorbates with very different wetting characteristics: specifically, one of the two components was terminated by a methyl group ($X = CH_3$, forming a hydrophobic, oleophobic monolayer) and the other by a polar or polarizable group (yielding a hydrophilic or oleophilic monolayer). In these systems the contact angles of water and hexadecane (HD) provided a qualitative indication of the composition of the monolayer. In general, the contact angle (or, more precisely, its cosine, since cos θ, not θ itself, is related to surface free energies[14]) is not linearly dependent on the composition of the surface[15] and hence

cannot easily be used for quantitation. Deviations from linearity do, however, provide valuable information on the structure of the monolayer and the extent of phase-segregation of the two components.

The self-assembly of monolayers on gold is driven by the formation of strong, coordinative gold-sulfur bonds. The chemistry of the thiol group does not limit our choice of substrate to gold. In fact, thiols self-assemble on many other metal surfaces, including platinum,[16] copper[17] and silver.[8] The monolayers formed on these metals may, due to the hardness of the substrate, stability of the monolayers, or orientation of the hydrocarbon chains, be more useful than monolayers on gold in some applications. For fundamental studies of organic surfaces, however, gold is an excellent substrate. High-purity gold is readily available and evaporates easily to form thin, uniform films.[18] The low reactivity of gold towards most organic functionalities provides great latitude in the range of tail groups that may be expressed at the surface. The lack of a stable gold oxide[19] obviates the need for special handling procedures and simplifies analysis by ellipsometry (the optical constants of the substrate are stable) and X-ray photoelectron spectroscopy (there is no oxide layer to interfere with quantitation of the photoelectrons from the substrate or from oxygen-containing functional groups).

We believe[9,20,21] that the species ultimately formed on the gold surface by adsorption of thiols from solution is a thiolate, RS^-. The mechanism by which an initially physisorbed thiol is converted to a chemisorbed thiolate remains unclear. In this paper we will use phrases such as "monolayer of an alkanethiol" to indicate the precursor from which the monolayer was formed, even though the actual species on the surface is probably a thiolate.

Thermodynamic v Kinetic Control over the Formation of Monolayers. One of the enigmas in these studies — one for which we do not yet have a definitive resolution — is whether the compositions of monolayers adsorbed from solutions containing two or more thiols are determined by thermodynamic equilibrium between the

monolayer and the solution or by the kinetics of adsorption. This question is made more complex by two observations that, at first sight, are mutually inconsistent. Most of the data in this and the following paper can be rationalized if the compositions of the mixed monolayers were at, or near, the values we would expect from thermodynamic equilibrium between the components of the monolayer and the adsorption solutions. It is difficult to construct a purely kinetic mechanism that accounts for the observed compositions. For example, a monolayer adsorbed from a mixture of two linear thiols with the same chain length may be composed almost exclusively of the minor species in solution, even when there is no obvious kinetic preference for one species over the other. Similarly, long-chain thiols were adsorbed preferentially over shorter chains, a preference which is antithetical to our intuition based on diffusion rates and steric hindrance. The presumption of thermodynamic equilibrium requires that a mechanism exist for reversible interchange of the components of the monolayer with those in solution at some time during the formation of the monolayer. Here a problem arises. The rate of desorption of molecules into solution from fully formed monolayers at room temperature is negligible, so equilibrium can not be established by desorption and readsorption of monolayer components in the complete monolayer. Similarly, displacement of components in a preformed monolayer by thiols in solution (Fig. 1) is too slow to account for the rapid equilibration (within, at most, a few seconds) required to explain the experimental results: after 12 hours of immersion in a 1 mM solution of $HS(CH_2)_{10}X$, less than half of a preformed monolayer of $HS(CH_2)_{10}Y$ (X, Y = CH_3, CH_2OH and vice versa) had been replaced by $HS(CH_2)_{10}X$.[22] With monolayers composed of longer chains, displacement was even slower.

This apparent paradox could be resolved if rapid equilibration were to occur at short times through some mechanism that was not available in the fully formed monolayer. One can postulate several possibilities. First, equilibration could proceed through the physisorbed thiol. We would expect similar enthalpic and entropic factors to influence the composition and distribution of the components in a monolayer of physisorbed thiols as in

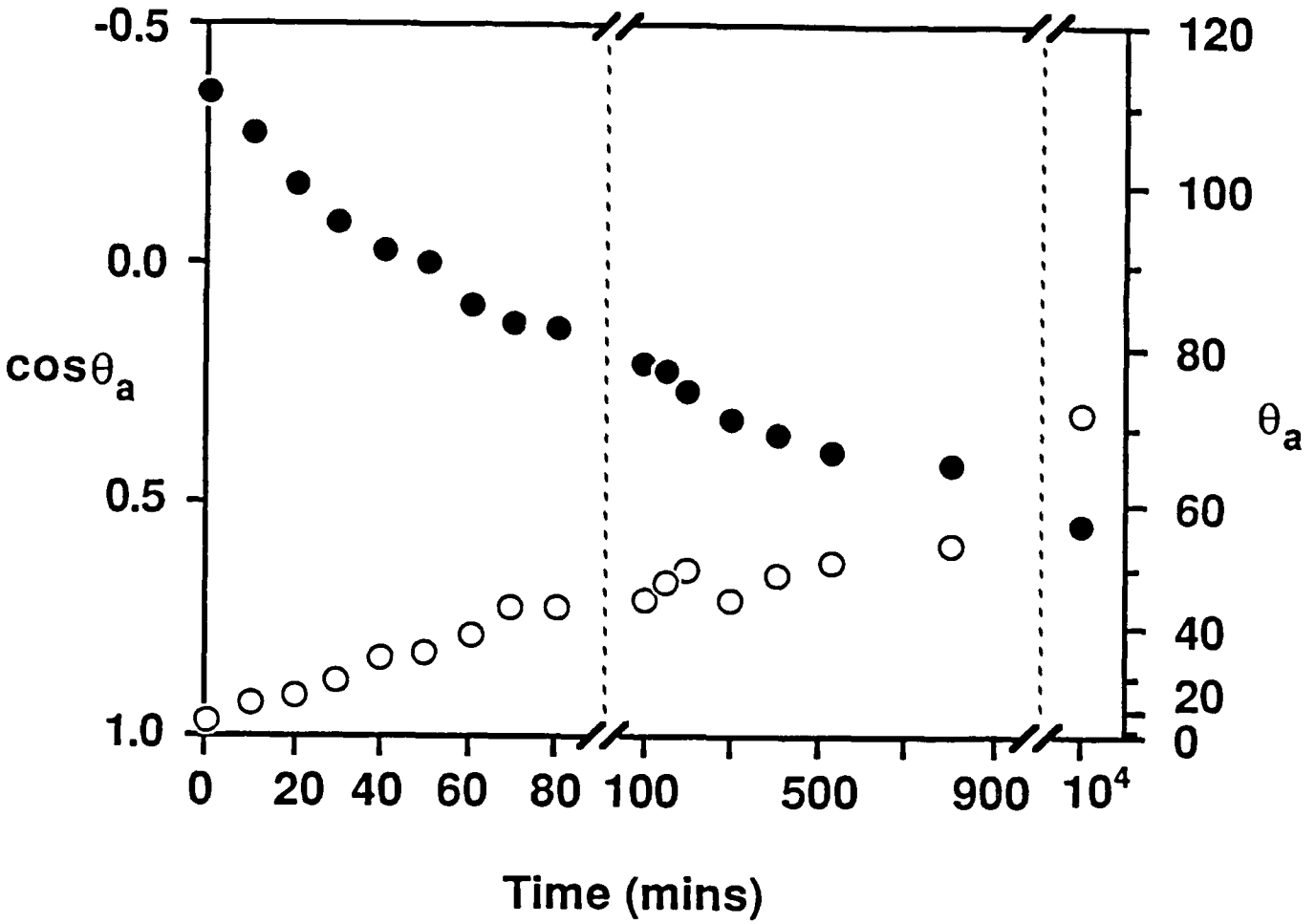

Figure 1. Displacement of monolayers of thiols on gold. Advancing contact angle of water as a function of the time of immersion of a preformed monolayer of $HS(CH_2)_{10}CH_3$ in a 1mM solution of $HS(CH_2)_{10}CH_2OH$ in ethanol (filled circles), and of a preformed monolayer of $HS(CH_2)_{10}CH_2OH$ in a 1 mM solution of $HS(CH_2)_{10}CH_3$ in ethanol (open circles). Note the change in the scale of the abscissa after 100 mins, and the axis break after 900 mins.

a monolayer of chemisorbed thiolates. In this scenario, rapid equilibration between the physisorbed thiol and the thiols in solution would be followed by relatively slow conversion of the physisorbed thiols to chemisorbed thiolates. If the rate constant for the conversion of thiol to surface thiolate were independent of the structure of the thiol, which is likely, a chemisorbed monolayer would be kinetically trapped with a composition equal to the equilibrium value in the physisorbed monolayer. Thus, even though the fully-formed monolayer does not equilibrate with the components in solution, equilibration through the physisorbed thiol would result in an equilibrium composition of the components in the monolayer. This mechanism is consistent with the observation that the activation barrier in UHV to desorption of a physisorbed thiol is lower than the barrier to chemisorption.[21] Equilibration during the early stages of monolayer formation could also conceivably proceed through the adsorbed thiolate. For example, the presence of surface hydrides (formed by dissociative chemisorption of the thiol) might be required for reversible adsorption. Surface hydrides would be lost rapidly as H_2[23] or H_2O, shutting down this mechanism and freezing in the equilibrium composition. A third possibility is that exchange between the monolayer and the solution is somehow mediated by unoccupied coordination sites on the gold. Clearly, it is important to determine the mechanism of adsorption and equilibration during the early stages of formation of a monolayer. As yet, however, we do not have firm evidence to support a particular mechanism, and we prefer not to speculate further.

Experimental Section

Materials. Ethanol (U.S. Industrials Co.) was deoxygenated with nitrogen before use. Hexadecane (Aldrich 99%), bicyclohexyl (Aldrich, 99%), decane (MCB) and isooctane (Fluka, HPLC grade) were slowly percolated twice through neutral, grade 1 alumina. Hexadecane and bicyclohexyl passed the Bigelow Test.[24] Acetonitrile (Aldrich,

gold label) was stirred over neutral, grade 1 alumina for 1 day and then distilled from calcium hydride. α-Bromonapthalene (Aldrich, 98%) was passed through silica gel and distilled from P_2O_5 in vacuo. Water was deionized and then distilled in a glass and Teflon still. Octylisonitrile (Dixon Fine Chemicals) was purified by flash chromatography on silica gel. Trioctylphosphine (Aldrich) was distilled in vacuo and stored under N_2. 11-Mercaptoundecanol, di(11-hydroxyundecyl) disulfide, diundecyl disulfide, 11-mercaptoundecanoic acid, 11-bromoundecanethiol, 9-mercaptononanonitrile, nonanethiol, undecanethiol, dodecanethiol, hexadecanethiol, nonadecanethiol, and docosanethiol were available from previous studies.[7,9]

19-Mercapto-1-nonadecanol ($HS(CH_2)_{18}CH_2OH$). A solution containing 50 mL of dry, distilled THF, 11 mL (60 mmol) of 1,8-dibromooctane (Aldrich, 98%) and 5 mL of 0.1 M Li_2CuCl_4 in THF was cooled to 0 °C under N_2. To this solution was added dropwise 85 mL of a 0.47 M solution of 10-undecenylmagnesium bromide over a period of 5 h. The deep purple solution was stirred for a further hour at 0 °C, warmed to room temperature, and quenched with 75 mL of sat. aq. NH_4Cl. After standing for several hours a clear, colorless supernatant and a blue aqueous phase developed. The organic layer was decanted and the aqueous layer extracted with ether (2 x 50 mL). The organic fractions were combined, washed with brine (2 x 50 mL), dried over $MgSO_4$ and concentrated on a rotary evaporator. Distillation (132–140 °C, 0.1 Torr) yielded 7.45 g of crude 19-bromo-1-nonadecene as a low melting white solid.

Disiamylborane was produced by addition of 6 mL of 2 M 2-methyl-2-butene in THF (Aldrich) to 6 mL of 1 M BH_3.THF at 0 °C. The solution was warmed to room temperature, cooled back to 0°C and 1.7 g (5 mmol) of 19-bromo-1-nonadecene added. Sodium hydroxide (2 mL, 1 N) and hydrogen peroxide (2 mL, 30 % in water) were added to the cooled solution. The solution was allowed to warm to room temperature and was then extracted with methylene chloride (2 x 10 mL). Washing with water, drying over $MgSO_4$ and removal of the solvent yielded a 1.86 g of a white solid. Recrystallization

from ethanol, flash chromatography with 3:1 hexane/ethyl acetate (Silica Gel 60, Merck) and a second recrystallization from hexane yielded 0.8 g of pure 19-bromo-1-nonadecanol as white needles (mp 74–75 °C).

To 25 mL of degassed, anhyd methanol were added 43 mg (1.9 mg-atom) of sodium, 0.134 mL (1.9 mmol) of thiolacetic acid (Aldrich, distilled) and 400 mg (1.1 mmol) of 19-bromo-1-nonadecanol. The solution was heated at reflux for 2 h under N_2 and then cooled to room temperature. Acetyl chloride (2 mL) was added and the solution heated at reflux for a further 15 min. The solution was cooled to room temperature and 5 mL of distilled water were added to dissolve salts. A white solid was recovered by filtration, washed with cold methanol, and recrystallized from hexane to yield 260 mg of 19-mercapto-1-undecanol as white plates. mp 67-68 °C; ^{1}H NMR ($CDCl_3$) δ 3.6 (t, 2 H), 2.5 (q, 2 H), 1.5–1.7 (m, 4 H), 1.3 (t, 1 H), 1.2–1.4 (m). Anal. Calcd (Found) for $C_{19}H_{40}OS$: C, 72.08 (72.13); H, 12.73 (12.89).

Preparation of Gold Substrates. A thermal evaporator operating at 10^{-6}–10^{-7} Torr was used to deposit 50 Å of chromium and 1000–2000 Å of gold (99.99%) onto polished (111) silicon wafers (Monsanto). The wafers were stored in polypropylene containers (Fluoroware) and cut into smaller slides (1 cm x 3 cm) before use.

Formation of Monolayers. Glassware was cleaned by heating for 1 h in 'piranha' solution (7:3 conc. H_2SO_4/30% H_2O_2 at 90 °C) followed by exhaustive rinsing with distilled water, a final rinse with absolute ethanol, and drying in an oven. Caution: 'piranha' solution reacts violently with most organic materials and must be handled with extreme care. Adsorption solutions containing two thiols were prepared in glass weighing bottles by diluting 4 mM stock solutions from 25-mL volumetric flasks. The accuracy of the concentrations of the stock solutions was limited by the analytical balance used to weigh solid adsorbates: estimated limits of error = ±5%. The transfers were carried out in gas-tight syringes under air. The transfer procedure may introduce errors up to ±0.01 in the mole fraction. The total concentration of thiol in solution was 1 mM. In solutions

containing disulfides, each molecule of the disulfide was counted twice so that the total concentration of sulfur-terminated alkyl chains in solution was 1 mM. Fresh solutions were always employed. Gold slides were washed with ethanol, blown dry with a stream of argon and immersed in the solutions overnight at room temperature.

Ellipsometry. Ellipsometric measurements were made on a Rudolf Research Type 43603-200E Ellipsometer using a wavelength of 6328 Å (He-Ne laser) and an incident angle of 70°. Details of the measurement procedure have been given previously.[9] The observed scatter in the data was typically ± 2 Å, arising largely, we believe, from differences in the amount of adventitious material adsorbed on the bare gold substrates before formation of monolayers.

Contact Angles. Contact angles were determined by the sessile drop technique on a Rame-Hart Model 100 Goniometer at room temperature and 100 % relative humidity for water, and ambient humidity for other liquids. Advancing contact angles, θ_a, were measured by forming a 1-μl drop (2 μl for angles over 80°) at the end of a PTFE-coated, blunt-ended needle, lowering the drop to the surface and removing the needle. Maximum advancing and minimum receding contact angles were measured using the technique of Dettre and Johnson.[25]

X-ray Photoelectron Spectroscopy. XPS spectra were obtained on an SSX-100 spectrometer (Surface Science Instruments) equipped with an Al Kα source, quartz monochromator, concentric hemispherical analyzer operating in fixed analyzer transmission mode, and multichannel detector. The take-off angle was 35° and the operating pressure was about 10^{-9} Torr. Acquisition times were sufficiently short that errors due to X-ray-induced damage were small.[26] The seven or eight samples in each experiment were mounted simultaneously on a multi-sample stage and analyzed sequentially using the automatic rotation facility. Samples were not focussed individually. Variations in the vertical position of the sample with respect to the focal plane of the spectrometer introduced a random error into the peak areas of approximately 3%. All spectra were referenced to

Au($4f_{7/2}$) at 84.00 eV. Spectra of O(1s), N(1s) and Br($3p_{3/2}$) used to quantitate the composition of the monolayer were acquired with a 100-eV pass energy, 1-mm spot size, 200-W anode power, and 15–30 scans (approximately 20–40 mins acquisition time). The O(1s), N(1s) and Br($3p_{3/2}$) signals were fitted with single 80% Gaussian/ 20% Lorentzian peaks, which were good approximations to the peak shapes on the monolayers with χ^p = 1.0. To calculate the composition of the monolayer, the area of the residual signal (if any) from the heteroatom on the pure methyl-terminated monolayer was subtracted from the areas of the peaks from the monolayers containing the heteroatom. These areas were normalized to the corrected area from the pure monolayer derived from $HS(CH_2)_nX$. The amount of oxygen, nitrogen or bromine in the monolayer can also be determined by subtracting the spectrum obtained on the pure methyl-terminated monolayer from the other spectra before fitting the peaks. This procedure leads to a flat baseline, which aids background subtraction, but also increases the noise by 40% and hence increases the fitting errors. Compositions calculated by this technique for the OH/Me monolayers adsorbed from ethanol agreed to within 2% of a monolayer with those calculated from the unsubtracted peaks. The Au(4f) photoelectrons were detected under the same conditions as the heteroatoms, but with only 2 scans. Both peaks were fit using a Shirley background subtraction[27] and a 80% Gaussian/ 20% Lorentzian peak shape, but only the area of the Au($4f_{7/2}$) peak was used for quantitation. The C(1s) peak from the mixed CO_2H/Me monolayers was acquired with a 50-eV pass energy and 600-μm spot. A total of 30 scans (43 minutes) were accumulated, distributed between two areas of each sample to minimize the effects of beam-induced damage to the sample. The spectrum for the pure monolayer of undecanethiol was rescaled to the same maximum peak height as the main methylene peak in each of the mixed monolayers, and subtracted from these spectra.[28] The high energy peak at 289.4 eV was then fit with a linear baseline and a single 90% Gaussian/ 10% Lorentzian peak constrained to a full width at half maximum of 1.45 eV (the width of the

peak from the pure acid-terminated monolayer). By choosing the limits of plausible choices for baselines, we estimated limits on fitting errors of ± 3% of a monolayer.

Results

Coordination to Gold. Although gold is unreactive compared to most metals, the gold surface is not entirely inert. A metastable surface oxide forms relatively easily[29] and surface hydrides can be formed at low temperatures, although H_2 is lost upon heating above 200 K.[23] Most small molecules (H_2S being a notable exception[30]), however, are only physisorbed to the gold surface and desorb below room temperature.[31] Self-assembled monolayers of alkyltrichlorosilanes have been formed on gold,[32] but there is no evidence of a specific chemical interaction with the gold surface. The gold merely provides a smooth substrate: the structural strength of the monolayer is provided by cross-linking of the siloxane head groups. Gold has also been used as a flat substrate for Langmuir-Blodgett monolayers,[33] but no studies have been conducted with head groups that bind specifically to the gold. Our interest lies principally in monolayers that are pinned to the gold surface by covalent chemical bonds, that are stable at room temperature in the absence of an incident flux of the adsorbate molecules, and that are robust enough to withstand washing and contact with water and a range of organic solvents.

Potential head groups can be divided into two broad categories: those that contain sulfur and those that do not. We have surveyed a number of long-chain compounds in the second category for their ability to form monolayers on gold from dilute solutions in ethanol (with the exception of trihexadecyl phosphine which was adsorbed from acetonitrile). The rationale for this survey is partly to find other stable monolayer systems and partly to determine whether particular tail groups are likely to compete strongly with a thiol in binding to the gold. Our criteria were that the monolayers be stable to washing with ethanol and have advancing contact angles, θ_a, that are indicative of a relatively well-

packed monolayer: for long-chain, methyl-terminated adsorbates $\theta_a(H_2O) > 100°$, $\theta_a(HD) > 40°$. Stearamine, heptadecanol, stearic acid,[34] stearamide, stearonitrile, 1-bromodocosane, ethyl hexadecanoate and didodecynyl mercury did not meet these criteria (Table I). Tricosyl isonitrile formed a stable monolayer with a thickness close to that expected for a monolayer oriented approximately normal to the surface, but the contact angles of water and hexadecane were substantially lower than on monolayers of alkanethiols. Of the molecules surveyed only trihexadecyl phosphine passed all these tests. The phosphorus signal in XPS was too weak to be observed easily in this monolayer. In a monolayer of trioctyl phosphine an unresolved doublet arising from the P(2p) photoelectrons was observed at a binding energy of 131.7 eV,[35] confirming the presence of a phosphine in the monolayer.[36]

A gold slide was immersed in a solution containing a 3:1 mixture of trioctyl phosphine and 11-hydroxyundecanethiol in acetonitrile in order to determine the relative affinity of thiols and phosphines for gold. The contact angle of water on the resulting monolayer was 47°, suggesting approximately equal amounts of polar hydroxyl and nonpolar methyl or methylene groups at the surface (vide infra). If the composition of the monolayer were the same as the solution, we would observe a 9:1 ratio of methyl to hydroxyl groups at the surface of the monolayer. Although a slight preference (< 2:1) for the adsorption of the thiol is expected based simply on the difference in chain lengths (see companion paper), the stronger preference observed suggests that adsorption of thiols is slightly favored over phosphines. We have not performed experiments to determine whether the composition of the mixed monolayer is under thermodynamic or kinetic control, or determined whether the preference for the thiol varies with adsorption conditions.

It is known from electrochemical studies that isonitriles coordinate to gold.[37] The contact angles on a monolayer formed from tricosyl isonitrile suggest that these monolayers are poorly packed compared to monolayers of thiols or phosphines. Thiols are adsorbed

Table I. Adsorption of Terminally-Functionalized Alkyl Chains from Ethanol onto Gold

	$\theta_a(H_2O)$[a]	$\theta_a(HD)$[b]	Thickness (Å)	
			Obsd[c]	Calcd[d]
$CH_3(CH_2)_{17}NH_2$	90	12	6	22–24
$CH_3(CH_2)_{16}OH$	95	33	9	21–23
$CH_3(CH_2)_{16}CO_2H$	92	38	7	22–24
$CH_3(CH_2)_{16}CONH_2$	74	18	7	22–24
$CH_3(CH_2)_{16}CN$	69	0	3	22–24
$CH_3(CH_2)_{21}Br$	84	31	4	28–31
$CH_3(CH_2)_{14}CO_2Et$	82	28	6	[h]
$[CH_3(CH_2)_9C{\equiv}C]_2Hg$	70	0	4	17–19
$[CH_3(CH_2)_{15}]_3P$[e]	111	44	21	21–23
$CH_3(CH_2)_{22}NC$	102	28	30	29–33
$CH_3(CH_2)_{15}SH$[f]	112	47	20	22–24
$[CH_3(CH_2)_{15}S]_2$	110	44	23	22–24
$[CH_3(CH_2)_{15}]_2S$[g]	112	45	20	22–24
$CH_3(CH_2)_{15}OCS_2Na$	108	45	21	24–26

[a] Advancing contact angle of water. [b] Advancing contact angle of hexadecane. [c] Computed from ellipsometric data using n = 1.45. [d] Assumes that the chains are close-packed, trans-extended and tilted between 30° and 0° from the normal to the surface. [e] Adsorbed from acetonitrile. [f] Ref. 9. [g] Ref. 7. [h] The large ester headgroup could not easily form a close-packed monolayer.

onto gold preferentially over isonitriles: a monolayer adsorbed from a 10:1 mixture of octyl isonitrile and 11-hydroxyundecanethiol in acetonitrile had a contact angle of 27° with water, an observation indicating that the thiol was the predominant component incorporated into the monolayer.

Given that "soft" nucleophiles such as phosphines and isonitriles coordinate to gold, it is not surprising that sulfur also binds well. The formation of self-assembled monolayers has been reported for several sulfur-containing molecules other than thiols, including disulfides (RSSR),[5,38] sulfides (RSR)[7,39] and thiophenes.[40,41] There exists some disagreement over the relative binding efficiencies of thiols and dialkyl sulfides. Troughton et al.[5] reported that when a dilute solution of a dialkyl sulfide in ethanol was doped to the extent of 1% with a thiol, a monolayer adsorbed from the solution had the same properties as a monolayer formed in a solution of the pure thiol. Monolayers of dialkyl sulfides were also thermally less stable than monolayers derived from thiols. These observations suggest that adsorption of thiols is strongly preferred over adsorption of sulfides. Rubenstein et al.[42] assumed, from indirect electrochemical evidence, that the composition of a monolayer adsorbed on a gold electrode from a solution containing an equimolar mixture of an alkyl thiol and a dialkyl sulfide reflected the composition of the solution. The actual composition of the monolayer was not determined, however, and the contact angles reported in the paper suggest that the monolayer consisted primarily of the thiol component.

We have studied the relative binding efficiencies of thiols and disulfides by adsorbing monolayers from solutions containing various mole fractions of $HS(CH_2)_{10}CH_2OH$ and $[S(CH_2)_{10}CH_3]_2$ in ethanol. The experiment was repeated with $HS(CH_2)_{10}CH_3$ and $[S(CH_2)_{10}CH_2OH]_2$ to enable us to eliminate the influence of the tail group on the adsorption process. Although we will present these experiments in detail elsewhere,[20] we summarize the results here (Figure 2). The compositions of the monolayers were determined from the intensity of the O(1s) photoelectron signal obtained

by XPS, normalized to the signal from a monolayer composed solely of the hydroxyl-terminated species. The disulfide was counted at twice its actual concentration in solution because each molecule contributes two chains to a monolayer. Figure 2 shows a strong preference (~75:1) for adsorption of the thiol, and a lesser predilection for adsorption of the methyl-terminated species. The data can be approximated by a constant preference for adsorption of the thiol independent of the ratio of thiol to disulfide in solution (straight lines in Figure 2).

Competitive Adsorption of Thiols with Different Tail Groups. To investigate the effect of the nature of the tail group on the coadsorption of thiols, we studied four two-component systems each composed of a methyl-terminated thiol and a thiol with a polar or polarizable tail group. Two of the tail groups were polar and capable of intramonolayer hydrogen-bonding (alcohol and carboxylic acid), one was dipolar aprotic (nitrile) and one was a highly polarizable group that does not form hydrogen bonds (bromide): $HS(CH_2)_{10}CH_3$ and $HS(CH_2)_{10}CO_2H$; $HS(CH_2)_{10}CH_3$ and $HS(CH_2)_{10}CH_2OH$; $HS(CH_2)_{10}CH_3$ and $HS(CH_2)_{10}CH_2Br$; $HS(CH_2)_8CH_3$ and $HS(CH_2)_8CN$. For each pair of compounds, a series of solutions were prepared in ethanol with a total concentration of 1 mM and varying mole fractions of the two components. Gold slides were immersed in these solutions overnight at room temperature and the monolayers were then analyzed by XPS and contact angle.

We assessed the reliability and accuracy of XPS for quantifying the composition of monolayers by determining the composition of mixed monolayers of $HS(CH_2)_{10}CO_2H$ and $HS(CH_2)_{10}CH_3$ in three different ways (Figure 3). First, the intensity of the O(1s) photoelectrons from each sample was normalized to the intensity of the O(1s) peak from the monolayer adsorbed from a solution containing only $HS(CH_2)_{10}CO_2H$.[43] Second, the ratio of the O(1s) intensity to the intensity of the $Au(4f_{7/2})$ photoelectrons from the substrate was used as a measure of the relative amount of acid-terminated thiol incorporated in the monolayer. The use of a ratio of the intensities of oxygen to gold eliminates errors

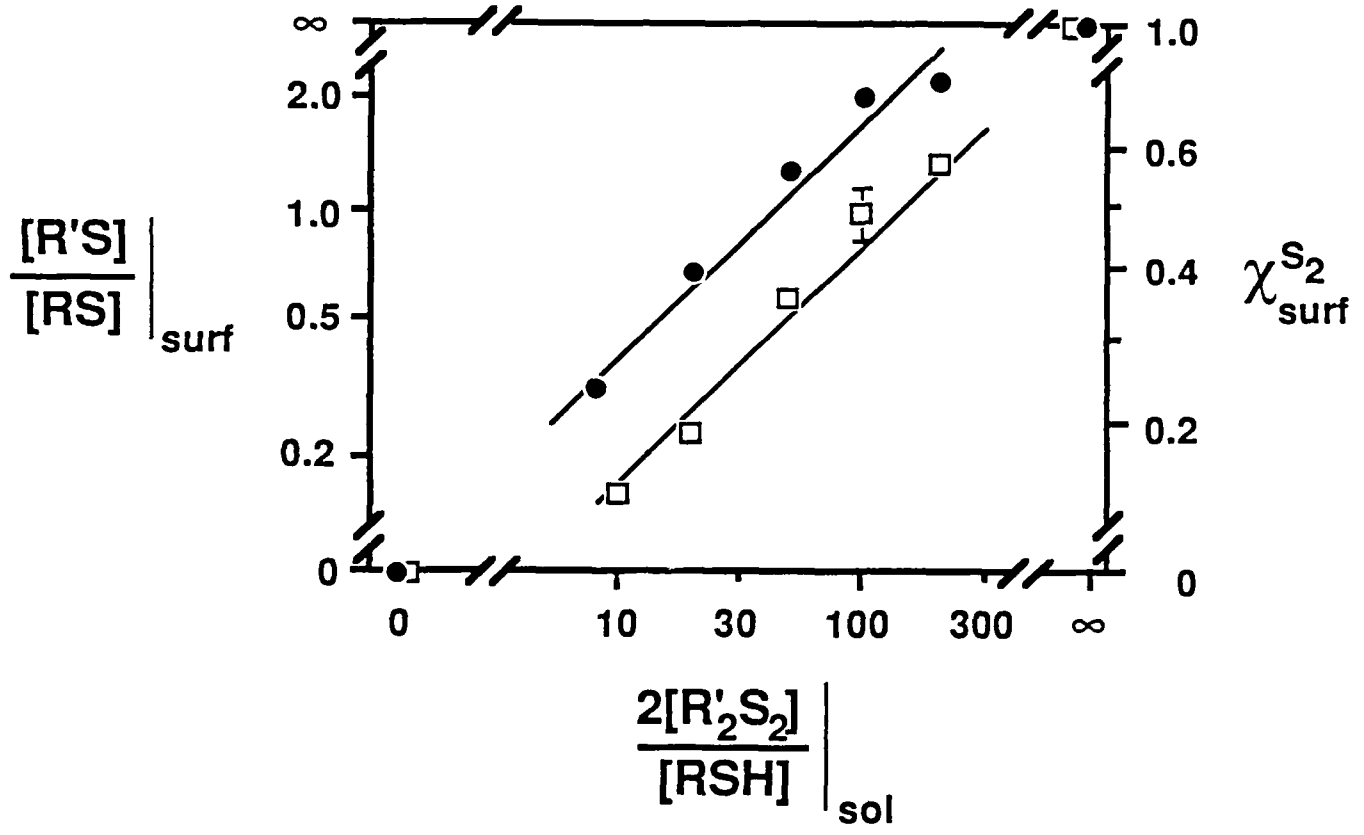

Figure 2. Composition of monolayers generated by the coadsorption from ethanol onto gold of $HS(CH_2)_{10}CH_3$ and $[S(CH_2)_{10}CH_2OH]_2$ (squares); and $HS(CH_2)_{10}CH_2OH$ and $[S(CH_2)_{10}CH_3]_2$ (circles). The ordinate represents the ratio of chains in the monolayer derived from the disulfide to those derived from the thiol, as determined by XPS. An estimated error bar (2σ) is shown. If there is a constant preference for adsorption of one species, independent of concentration, the data should fall on straight lines with a slope of one, such as those shown on the graph.

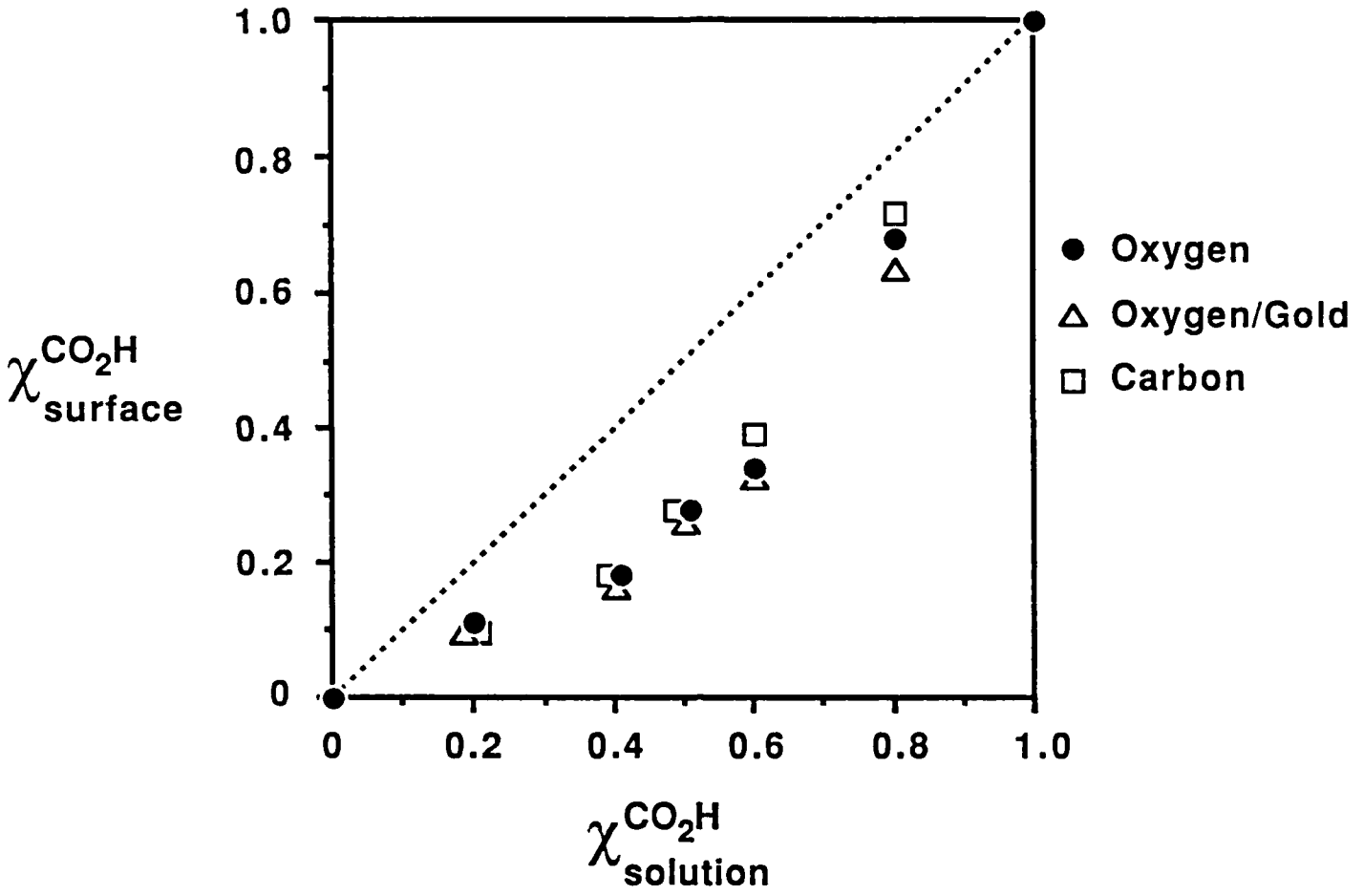

Figure 3. Mole fraction of $HS(CH_2)_{10}CO_2H$ in monolayers adsorbed on gold from mixtures of $HS(CH_2)_{10}CO_2H$ and $HS(CH_2)_{10}CH_3$ in ethanol. The composition of the monolayer was calculated from the intensities of the O(1s) photoelectrons (circles), the ratio of the O(1s) to the $Au(4f_{7/2})$ peaks (triangles), and the intensity of the C(1s) photoelectrons arising from the carboxylic acid group (squares).

arising from variations in the absolute intensity of the spectra. Such errors arise principally from small variations in the vertical position of the sample with respect to the focal point of the spectrometer, but could also arise from drift in the spectrometer performance during data acquisition (no such drift was observed during the acquisition of the data presented here). The draw-back of the second approach is that changes in attenuation of the substrate signal could introduce errors into the calculated compositions, for example, if the structure of the monolayer were to change with composition or if a sample were not absolutely level. If the O(1s) intensity is a good measure of the composition of the monolayer, it should be correlated with the intensity of the C(1s) peak arising from $\underline{C}O_2H$. If, for example, oxygen-containing contaminants are adsorbed strongly on the polar acid surfaces, it should be evident by comparing the intensities of the O(1s) and C(1s) photoelectrons. In general, the C(1s) peak is not a good choice for quantitation because the low atomic photoionization cross-section leads to poor signal-to-noise, the peaks arising from the functionalized carbon are often not well-resolved from the main methylene peak, and the baseline is not flat, making accurate background subtraction difficult. Here we have attempted to quantify the C(1s) peak at 289.3 eV in order to confirm the compositions calculated from the O(1s) peaks. Figure 3 shows that the agreement between these three calculations of the composition is remarkably good. The greatest disparities in absolute terms among the calculated compositions occur at large χ^{CO_2H} where the errors in the measurement of the 100% acid surface have the greatest effect on the calculated compositions.

The random error in data acquisition and peak-fitting was determined for monolayers adsorbed from a typical solution of 0.6 mM $HS(CH_2)_{10}CH_2OH$ and 0.4 mM $HS(CH_2)_{10}CH_3$ in ethanol. Eight gold slides adsorbed from the same solution were analyzed sequentially using a multi-sample stage under the same conditions used in the analysis of a series of samples of varying composition. The standard error in both the O(1s) intensity and O/Au ratio was 3%. The O(1s) and Au($4f_{7/2}$) intensities were partially correlated as expected if differences in the focus of the samples were a cause of variability

in the measured areas of the photoelectron peaks. The two samples that had the highest O(1s) intensities also had the highest Au($4f_{7/2}$) photoelectron intensities. The compositions of the monolayers presented in subsequent figures were calculated from the intensity of the O(1s), N(1s) or Br(3p) photoelectrons. On one occasion in which the Au($4f_{7/2}$) intensity was abnormally low (> 3σ deviation from the mean of the other samples within an experiment), the intensity of the photoelectrons from the heteroatom was corrected for the deviation in the gold intensity. This case arose in the Br/Me system, in which there was no plausible cause of the aberration other than instrumental factors. Typical XPS spectra of the O(1s) region are shown for $HS(CH_2)_{10}CH_2OH/HS(CH_2)_{10}CH_3$ in Figure 4. The spectra are plotted after subtraction of the spectrum obtained from the monolayer of pure undecanethiol. The dashed line shows the position of the peak maximum in the spectrum from the pure hydroxyl-terminated monolayer. A significant shift (~0.4 eV) to higher binding energy occurred as the concentration of hydroxyl groups in the monolayer decreased. This shift is not a consequence of differential charging between samples: the position of the Au($4f_{7/2}$) peak was constant to within ±0.01 eV.

Figure 5 presents the relationship between the composition of the solution[44] in ethanol and the composition of the monolayer for the four systems under study. Only in the mixed Me/Br system did the composition of the monolayer reflect the concentrations in solution: the surfaces of the other monolayers were methyl-rich. The advancing contact angles of water and hexadecane are shown in Figure 6 as a function of the mole fraction of the polar component in the monolayer, as determined by XPS. We remeasured the contact angles on the monolayers adsorbed from mixed solutions of $HS(CH_2)_{10}CH_2OH$ and $HS(CH_2)_{10}CH_3$ after immersion of the slides in the adsorption solutions for a further two months: the contact angles had not changed significantly.

For the OH/Me system we also measured the receding contact angles of water. Hysteresis (which we define here as the difference between the minimum receding contact angle and the maximum advancing contact angle, expressed as cosines: $\cos \theta_{r,min}$ - cos

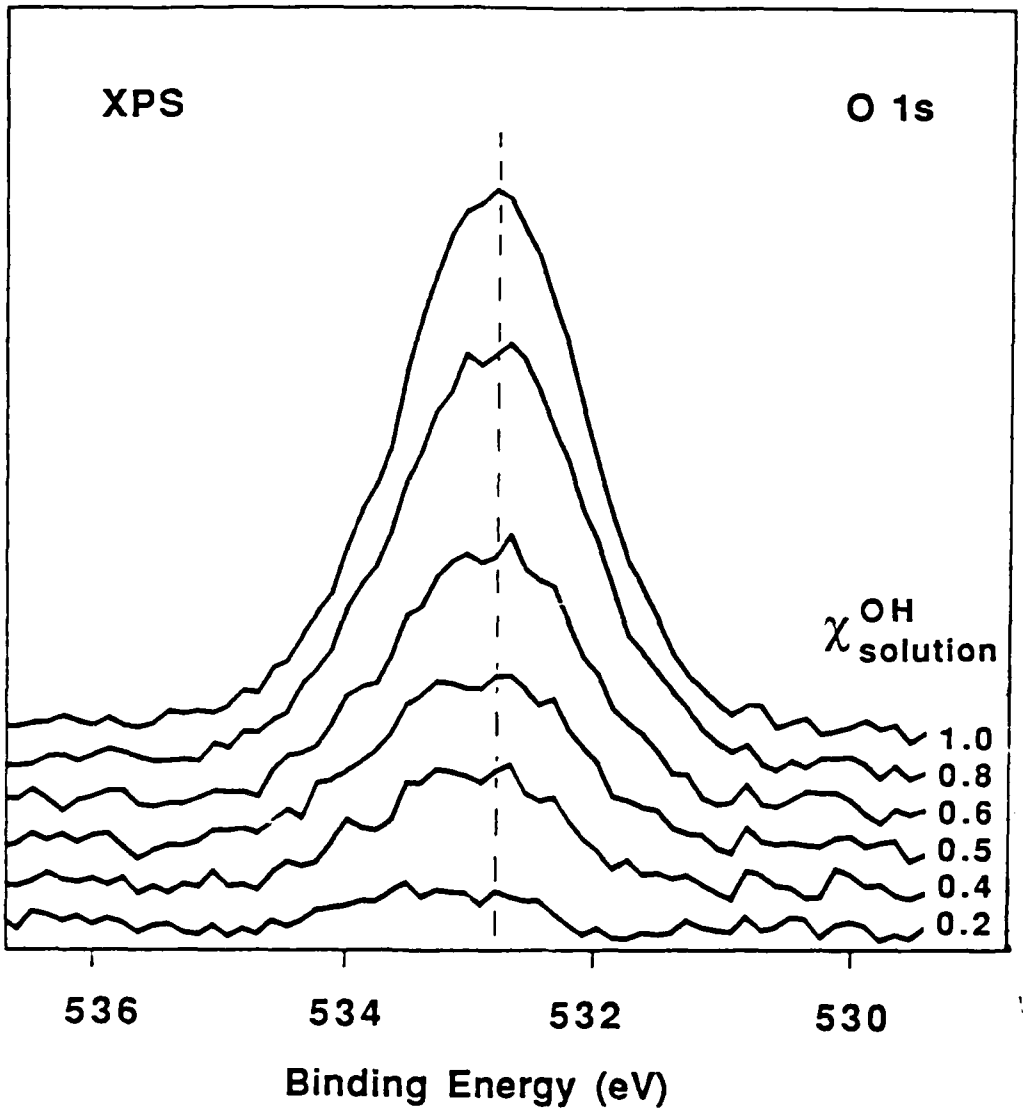

Figure 4. O(1s) peak in the XPS spectrum of monolayers adsorbed from mixtures of $HS(CH_2)_{10}CH_2OH$ and $HS(CH_2)_{10}CH_3$ in ethanol. The data were acquired with a pass energy of 100 eV and a spot size of 1 mm. The spectra are shown after subtraction of the background spectrum acquired on the pure $HS(CH_2)_{10}CH_3$ monolayer. The dashed line indicates the peak position for the monolayer of pure $HS(CH_2)_{10}CH_2OH$.

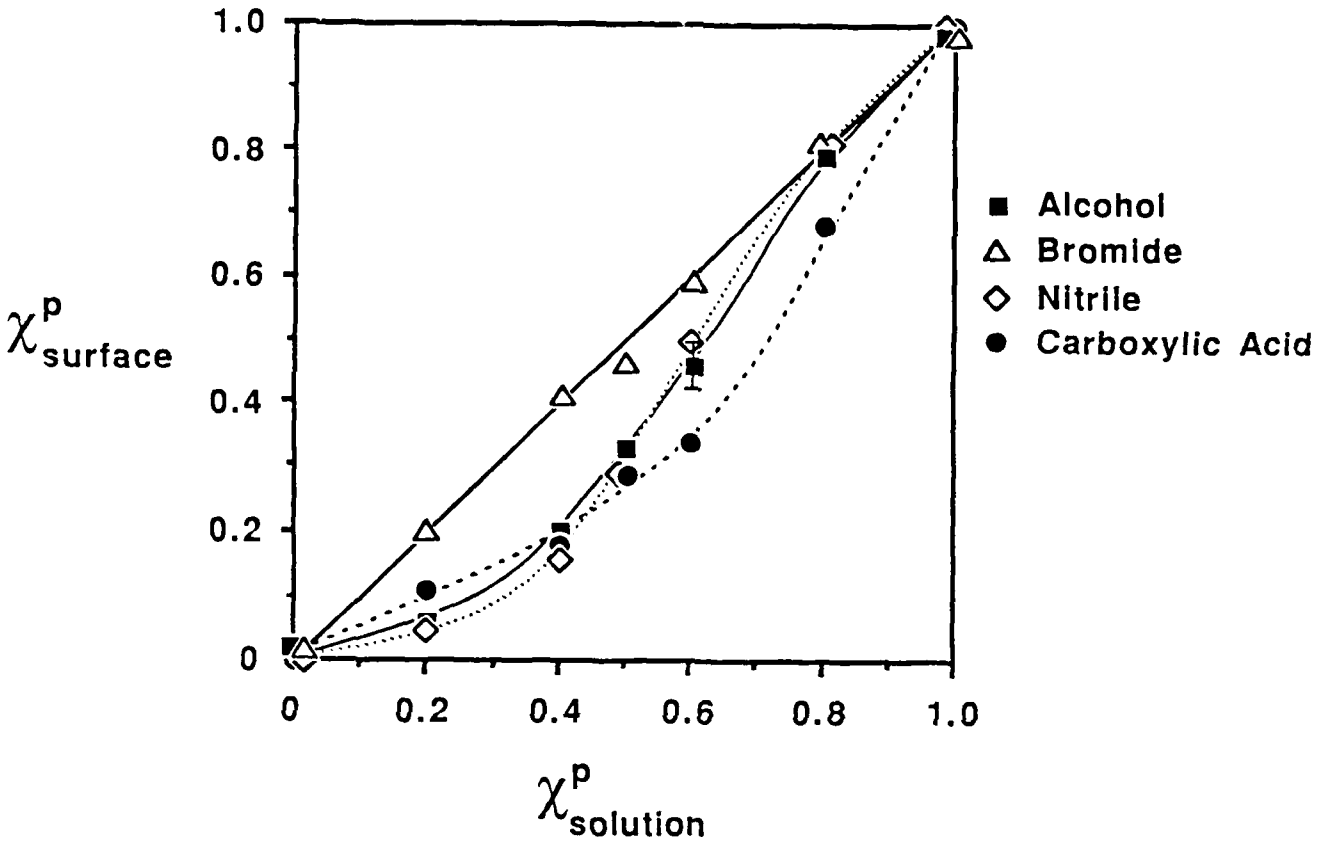

Figure 5. Composition of monolayers adsorbed from ethanolic mixtures of $HS(CH_2)_{10}CH_3$ and $HS(CH_2)_{10}CO_2H$ (circles); $HS(CH_2)_8CH_3$ and $HS(CH_2)_8CN$ (diamonds); $HS(CH_2)_{10}CH_3$ and $HS(CH_2)_{10}CH_2Br$ (triangles); and $HS(CH_2)_{10}CH_3$ and $HS(CH_2)_{10}CH_2OH$ (squares). χ^P represents the mole fraction of the polar-terminated species either in solution or on the surface. The solid and dashed lines are manual fits included simply as a guide to the eye. χ^p_{surf} was calculated from the intensity of the O(1s), N(1s) or Br(3d) photoelectrons. The error bar shown is representative of the random errors (2σ) involved in the analysis of the XPS data.

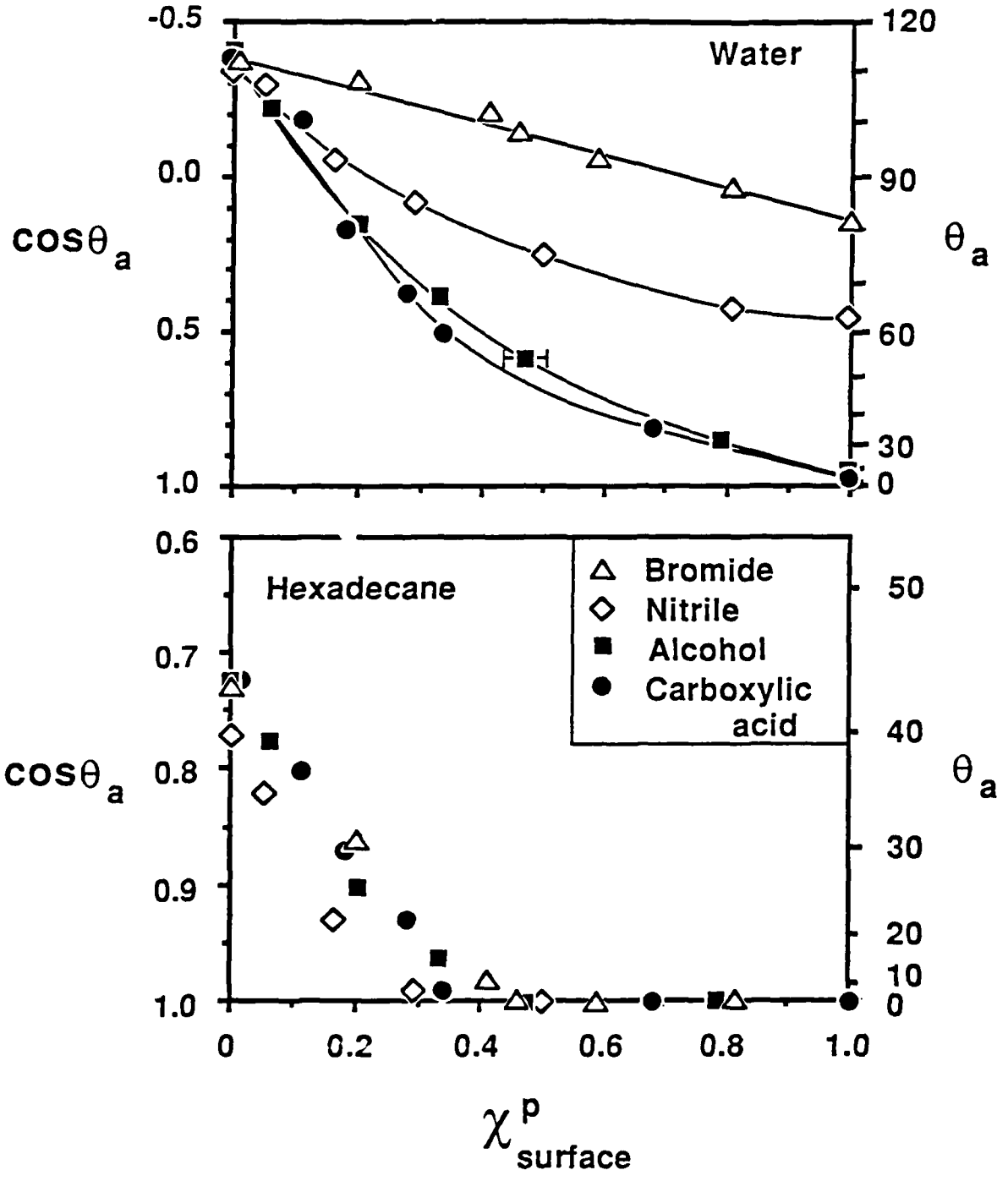

Figure 6. Advancing contact angles of water (upper figure) and hexadecane (lower figure) on monolayers adsorbed from ethanol onto gold slides: $HS(CH_2)_{10}CH_3$ and $HS(CH_2)_{10}CO_2H$ (circles); $HS(CH_2)_8CH_3$ and $HS(CH_2)_8CN$ (diamonds); $HS(CH_2)_{10}CH_3$ and $HS(CH_2)_{10}CH_2Br$ (triangles); and $HS(CH_2)_{10}CH_3$ and $HS(CH_2)_{10}CH_2OH$ (squares). Errors in contact angles lie within the symbols. A representative error (2σ) bar in χ^p_{surf} is shown. The lines in the upper figure are purely to assist the reader.

$\theta_{a,max}$) in heterogeneous systems is not well-understood, but does give some indication of the distribution of the two adsorbates within the monolayer. If the two components segregated into macroscopic domains (vide infra), the nonpolar islands would pin the edge of a drop of water advancing across the surface and the polar islands would pin the edge of a receding drop. Consequently, the hysteresis would be much greater on the mixed surfaces than on monolayers comprising a single pure component. Figure 7 shows the maximum advancing and minimum receding contact angles of water on OH/Me surfaces. Neither the hysteresis in cos θ nor in θ was correlated with the composition or polarity of the surface. Hysteresis on the mixed surfaces was only slightly greater than on the pure methyl surface. This result agrees with a previous study,[45] which showed that the hysteresis in the contact angles of water at pH = 3 (so as not to ionize the carboxylic acids) on mixed monolayers of $HS(CH_2)_{15}CO_2H$ and $HS(CH_2)_{15}CH_3$ was independent of the composition of the monolayer in the regime where the receding angle was nonzero.

The chain lengths in these studies were chosen largely on grounds of solubility and ease of synthesis. Other studies[7,46] have shown that nine and eleven-carbon chains are in a transitional regime between the longer chains, where the properties of the monolayer are largely independent of chain length, and shorter chains where the wettability and the structure of the monolayers vary with chain length. It is important to show that the results obtained here are not an artifact of working in this transitional regime but also hold for longer chains. Figure 8 compares the composition of the monolayer and the contact angles obtained for $HS(CH_2)_{10}CH_2OH/HS(CH_2)_{10}CH_3$ and the nineteen-carbon analogues $HS(CH_2)_{18}CH_2OH/HS(CH_2)_{18}CH_3$. Qualitatively the results are indistinguishable. Quantitatively, the differences are largely within the errors in the measurements and do not show any consistent trend that might indicate changes in the structure of the monolayer or in the energetics of the adsorption process. The advancing contact angles of water published previously[45] for mixed monolayers of $HS(CH_2)_{15}CO_2H$ and $HS(CH_2)_{15}CH_3$

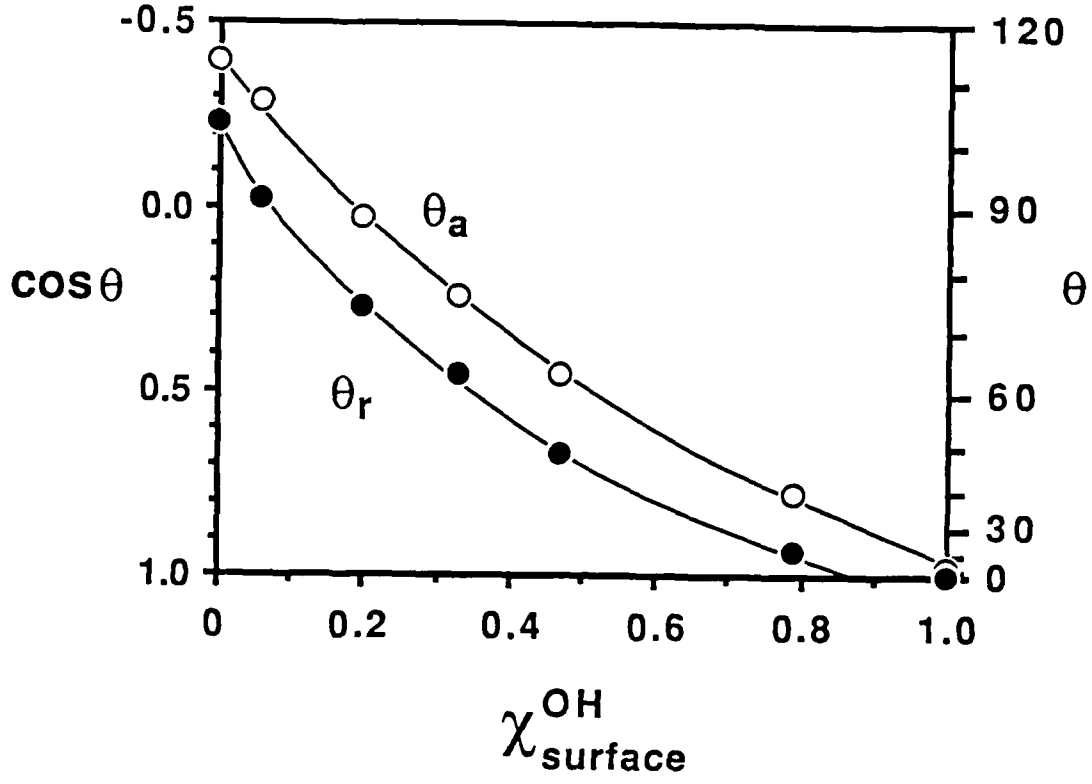

Figure 7. Maximum advancing (open circles) and minimum receding contact angles (filled circles) on gold slides after immersion for 2 months in solutions containing mixtures of $HS(CH_2)_{10}CH_3$ and $HS(CH_2)_{10}CH_2OH$.

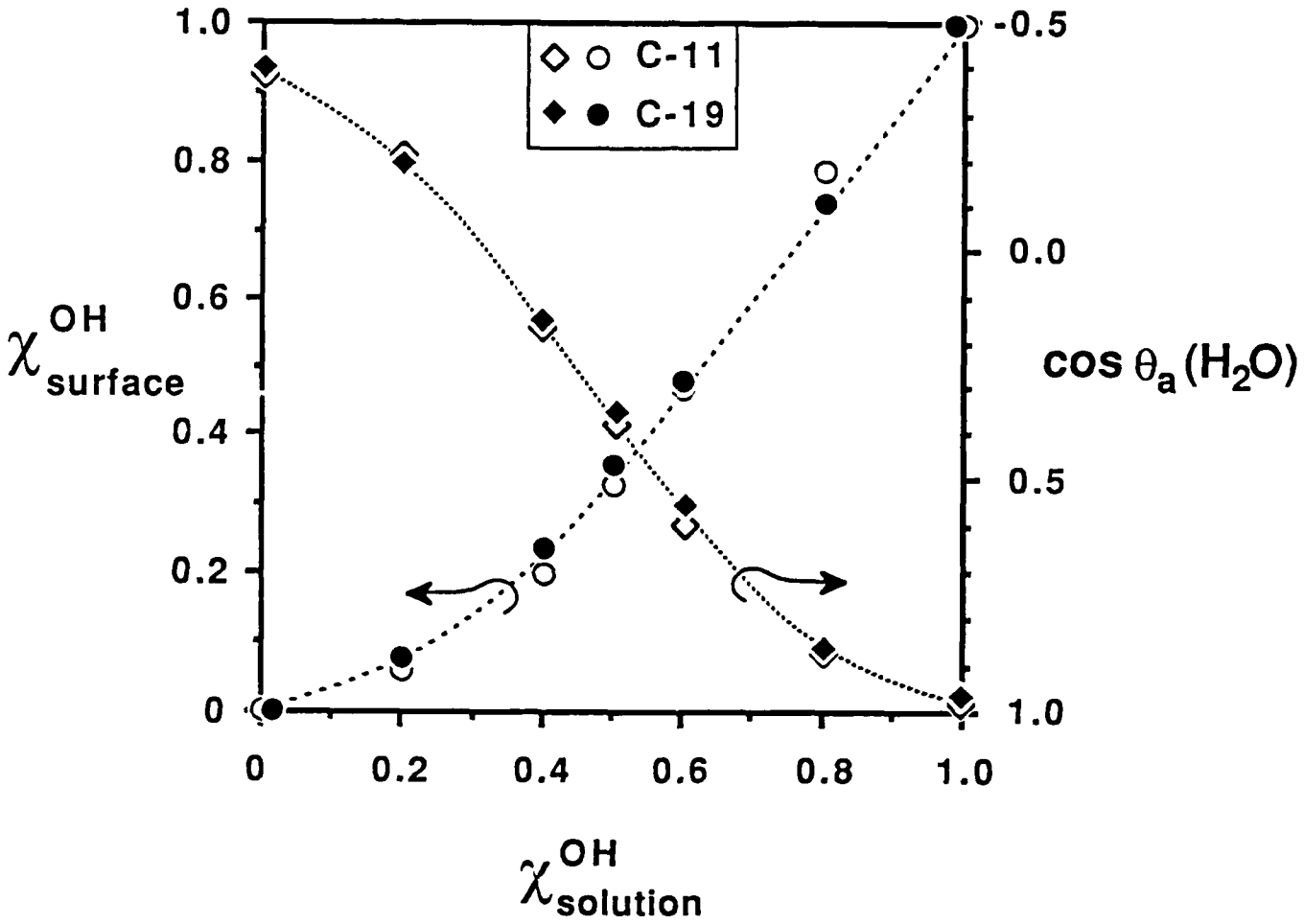

Figure 8. Comparison of monolayers formed by immersion of gold slides in ethanolic solutions containing mixtures of $HS(CH_2)_{10}CH_3$ and $HS(CH_2)_{10}CH_2OH$ (open symbols), and mixtures of $HS(CH_2)_{18}CH_3$ and $HS(CH_2)_{18}CH_2OH$ (solid symbols) for 12-24 hours: mole fraction of the alcohol-terminated thiol in the monolayer (circles), and advancing contact angles of water (diamonds).

are also in qualitative agreement with the results reported here for $HS(CH_2)_{10}CO_2H$ and $HS(CH_2)_{10}CH_3$.

Influence of Solvent on Adsorption. The nature of the adsorption solvent may influence the composition and structure of a monolayer in several ways. If the components of the monolayer are at, or near, thermodynamic equilibrium with the solution, then a change of solvent will change the activities of the adsorbates in solution and hence change the equilibrium composition of the monolayer. The solvent may be incorporated into the adsorbed monolayer.[47] This problem is likely to be particularly acute if there is geometrical matching between the solvent and the components of the film e.g. linear, long-chain adsorbates in hexadecane. Finally, if the tail groups are capable of strong specific interactions, particularly hydrogen bonding, then interactions among the tail groups and between the tail groups and the solvent will control the structure of the monolayer-liquid interface and may affect the structure of the bulk of the monolayer itself.

Gold slides were immersed in solutions containing mixtures of $HS(CH_2)_{10}CH_2OH$ and $HS(CH_2)_{10}CH_3$ in a polar, protic solvent (ethanol), a polar, aprotic solvent (acetonitrile), and a nonpolar solvent (isooctane). Figure 9 plots the area of the O(1s) photoelectron peak (normalized to the monolayer adsorbed from a solution of pure 11-hydroxyundecanethiol) and the advancing contact angles of water against the mole fraction of 11-hydroxyundecanethiol in *solution*. In acetonitrile the mole fraction of the alcohol in the monolayer varied smoothly with the composition of the solvent but was greater than with ethanol as solvent. In both ethanol and acetonitrile, XPS (through attenuation of the photoelectrons from the gold) and ellipsometry indicated no significant variation in the thickness of the monolayer as a function of composition. In addition, the contact angles on the monolayers adsorbed from ethanol and acetonitrile fall on the same line when plotted against the composition of the monolayer, except for the pure monolayer of $HS(CH_2)_{10}CH_2OH$ which was more hydrophilic when adsorbed from ethanol ($\theta_a(H_2O) < 10°$) than acetonitrile ($\theta_a(H_2O) = 19°$). In isooctane, monolayers adsorbed from two-

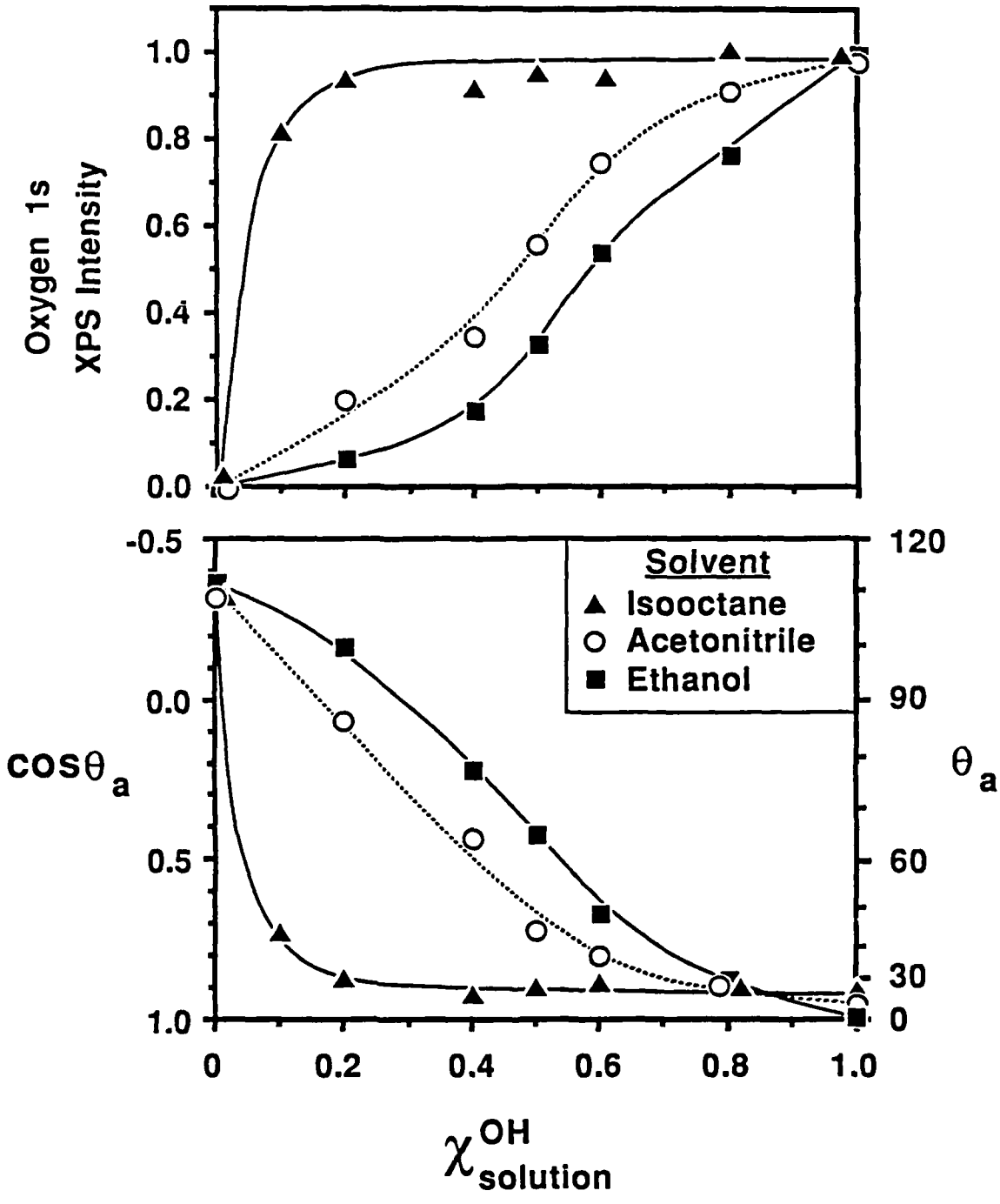

Figure 9. Comparison of monolayers adsorbed onto gold from mixtures of $HS(CH_2)_{10}CH_3$ and $HS(CH_2)_{10}CH_2OH$ dissolved in isooctane (triangles), acetonitrile (circles) and ethanol (squares). Intensity of the O(1s) photoelectron peak normalized to the monolayer adsorbed from a pure solution of $HS(CH_2)_{10}CH_2OH$ (upper figure); advancing contact angle of water (lower figure). The solid (ethanol, isooctane) and dotted lines (acetonitrile) are included simply as guides to the eye.

component solutions were composed almost exclusively of the hydroxyl-terminated thiol. Only in the most dilute solution (10% $HS(CH_2)_{10}CH_2OH$, 90% $HS(CH_2)_{10}CH_3$) did the intensity of the O(1s) peak in XPS or the contact angle of water indicate any incorporation of the methyl-terminated species. Ellipsometry and XPS suggested that the monolayers adsorbed from isooctane that comprised largely $HS(CH_2)_{10}CH_2OH$ were 2–4 Å thicker than the monolayer of $HS(CH_2)_{10}CH_3$. The contact angles of water (~25°) on the monolayers of $HS(CH_2)_{10}CH_2OH$ adsorbed from isooctane were also higher than those on monolayers adsorbed from ethanol and acetonitrile.

The nature of the solvent not only has a dramatic effect on the composition of the mixed monolayers but also appears to have more subtle effects on the structure of pure monolayers. Table II presents a comparison of monolayers of pure $HS(CH_2)_{10}CH_2OH$ and $HS(CH_2)_{10}CH_3$ adsorbed from ethanol, acetonitrile, isooctane and hexadecane. Hexadecane is a linear, rod-like monolayer that has the potential to interpenetrate with the hydrocarbon chains of the thiols. Isooctane is a small, globular molecule which is unlikely to be trapped within the monolayer. The extent of incorporation of solvent into these monolayers should be evident by comparing the data from these two alkanes.

The strong preference for adsorption of $HS(CH_2)_{10}CH_2OH$ from isooctane was remarkable. The kinetics of the adsorption process are shown in Figure 10 for a 4:1 mixture of $HS(CH_2)_{10}CH_3$ to $HS(CH_2)_{10}CH_2OH$. The predominance of the hydroxyl-terminated species in the monolayer was established at very short times: the first data point, taken by dipping the slide in the adsorbate solution and immediately rinsing it with clean ethanol, was already characteristic of a fairly polar surface despite the probable kinetic preference for the methyl-terminated thiol during the initial stage of adsorption onto clean gold.[48]

Table II. Properties of Monolayers of Thiols Adsorbed onto Gold from Different Solvents

Solvent	Thiol	XPS Peak Areas (Kcts) Au($4f_{7/2}$)	C(1s)	O(1s)	τ(Å)[a]	$\theta_a(H_2O)$[b]	θ_a(HD)[c]
Ethanol	$HS(CH_2)_{10}CH_2OH$	100	87	60	13	< 5	
Ethanol	$HS(CH_2)_{10}CH_3$	101	87		12	113	44
Acetonitrile	$HS(CH_2)_{10}CH_2OH$	98	91	66	17	10	
Acetonitrile	$HS(CH_2)_{10}CH_3$	98	90		18	112	44
Isooctane	$HS(CH_2)_{10}CH_2OH$	99	95	68	15	29	
Isooctane	$HS(CH_2)_{10}CH_3$	105	88		14	110	43
Hexadecane	$HS(CH_2)_{10}CH_2OH$	100	93	69	15	24	
Hexadecane	$HS(CH_2)_{10}CH_3$	105	86		13	110	43

[a] Ellipsometric thickness [b] Advancing contact angle of water [c] Advancing contact angle of hexadecane

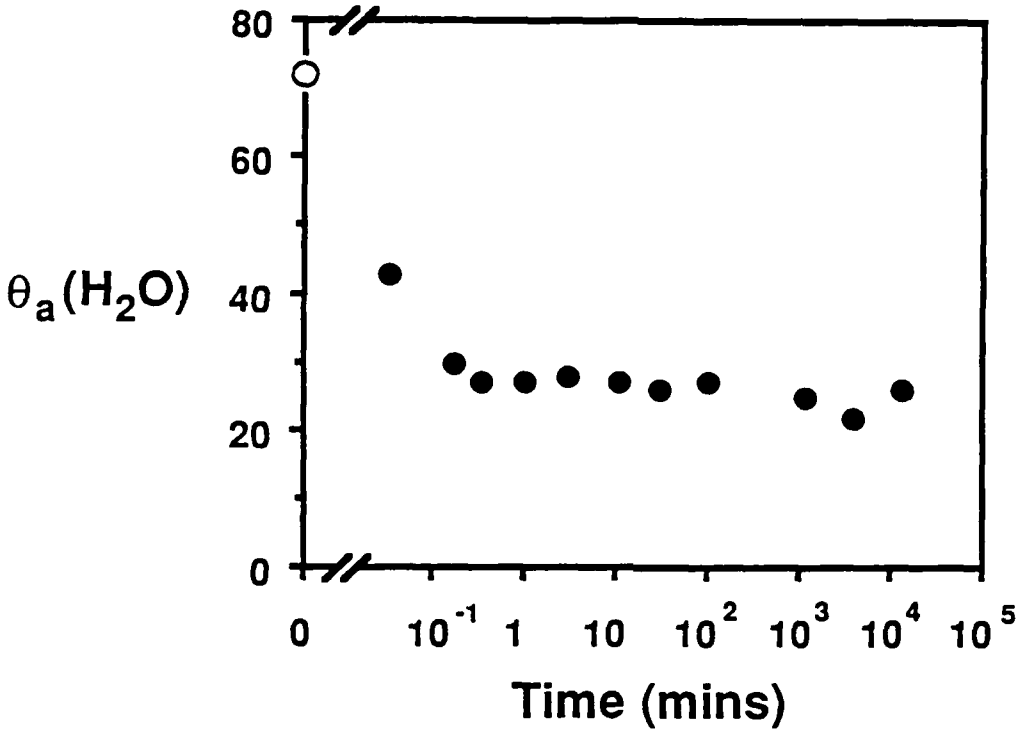

Figure 10. Advancing contact angle of water as a function of the time of immersion of a gold slide in a 1mM solution in isooctane containing a 4:1 mixture of $HS(CH_2)_{10}CH_3$ and $HS(CH_2)_{10}CH_2OH$. The open circle represents the contact angle of water on the gold slide before immersion in the solution of the thiols. The first data point shown by a filled circle was obtained by dipping the gold slide in the thiol solution, and immediately removing the slide and rinsing it with clean ethanol.

Discussion

Several species other than thiols, including disulfides, (RSSR), sulfides (RSR), and phosphines (R_3P), adsorb from solution and form stable monolayers on gold. Adsorption of thiols is preferred over these other adsorbates.[49] None of the other film-forming molecules surveyed formed a monolayer whose quality was clearly superior to that of a monolayer formed from a thiol and most, as indicated by contact angles, formed inferior monolayers. Dialkyl sulfides and substituted thiophenes offer greater electrochemical stability than thiols and, together with disulfides, allow one to introduce equal concentrations of two functional groups into the monolayer by using dissimilar chains. We have shown, however, that polyfunctional surfaces can also be constructed by competitive adsorption of thiols, with full control over the relative concentrations of the different components in the monolayer. Adsorption of thiols appears to be strongly favored over disulfides or sulfides from multi-component solutions, but only slightly favored over trialkyl phosphines. Control over the structure of the monolayer is most easily obtained if the same head group is employed for each component with changes introduced only in the chains and tail groups.

The composition of the monolayer adsorbed from a solution containing two thiols is not , in general, determined by a simple equilibrium expression. If the monolayer and the solution are in equilibrium then

$$RSH_{surf} + R'SH_{sol} \underset{}{\overset{K_{eq}}{\rightleftharpoons}} R'SH_{surf} + RSH_{sol} \qquad (1)$$

$$K_{eq} = \frac{[RSH]_{sol}[R'SH]_{surf}}{[RSH]_{surf}[R'SH]_{sol}} \qquad (2)$$

where K_{eq} would be constant if the monolayer were to act as an ideal two-dimensional solution. (The solutions were sufficiently dilute that the activity coefficients in solution may be assumed to be constant.) To a very rough approximation, the structure of the adsorbates in a pure monolayer is similar to that in a crystal of that component. We might thus expect K_{eq} to reflect the relative solubilities of the two components in the adsorption solvent. Figure 11 plots K_{eq}, calculated using equation 2 and the data from Fig. 5, against the mole fraction of the polar species in solution in ethanol. Only in the Br/Me system were the composition of the solution and the monolayer the same. Neither the Br nor CH_3 tail group has a strong specific interaction with the solvent.[50] Since there was no apparent preference for adsorption of either species we may infer an absence of strong specific interactions within the monolayer.

An alternative explanation for the correlation between the concentrations of $HS(CH_2)_{10}CH_2Br$ and $HS(CH_2)_{10}CH_3$ in solution and the composition of the monolayer could be that the compositions of the monolayers were determined kinetically by diffusion to the surface. In this case, we would expect K_{eq} to be independent of concentration for all the systems studied, with its value determined by the relative diffusion constants of the two species. This expectation is clearly not consistent with the variation in K_{eq} observed for the OH/Me and CN/Me systems. For the CO_2H/Me system adsorption of the methyl-terminated species was preferred at all concentrations, reflecting better solvation of the carboxylic acids in solution in ethanol than at the surface of the monolayer.[51]

The OH/Me and CN/Me systems are the most interesting. In both of these systems adsorption of the component with the polar tail group was strongly disfavored at low concentrations in solution, but Keq approached unity as χ^p approached one. This behavior is similar to that observed in regular solutions with an excess free energy of mixing $g^{excess} = \xi\chi^p\chi^{np}$, where ξ is a positive constant.[52] In solutions of n-alkanes and n-alcohols, breaking of hydrogen bonds leads to large positive excess enthalpies of mixing.[53] A similar effect in the monolayer might produce the adsorption isotherm obtained for the

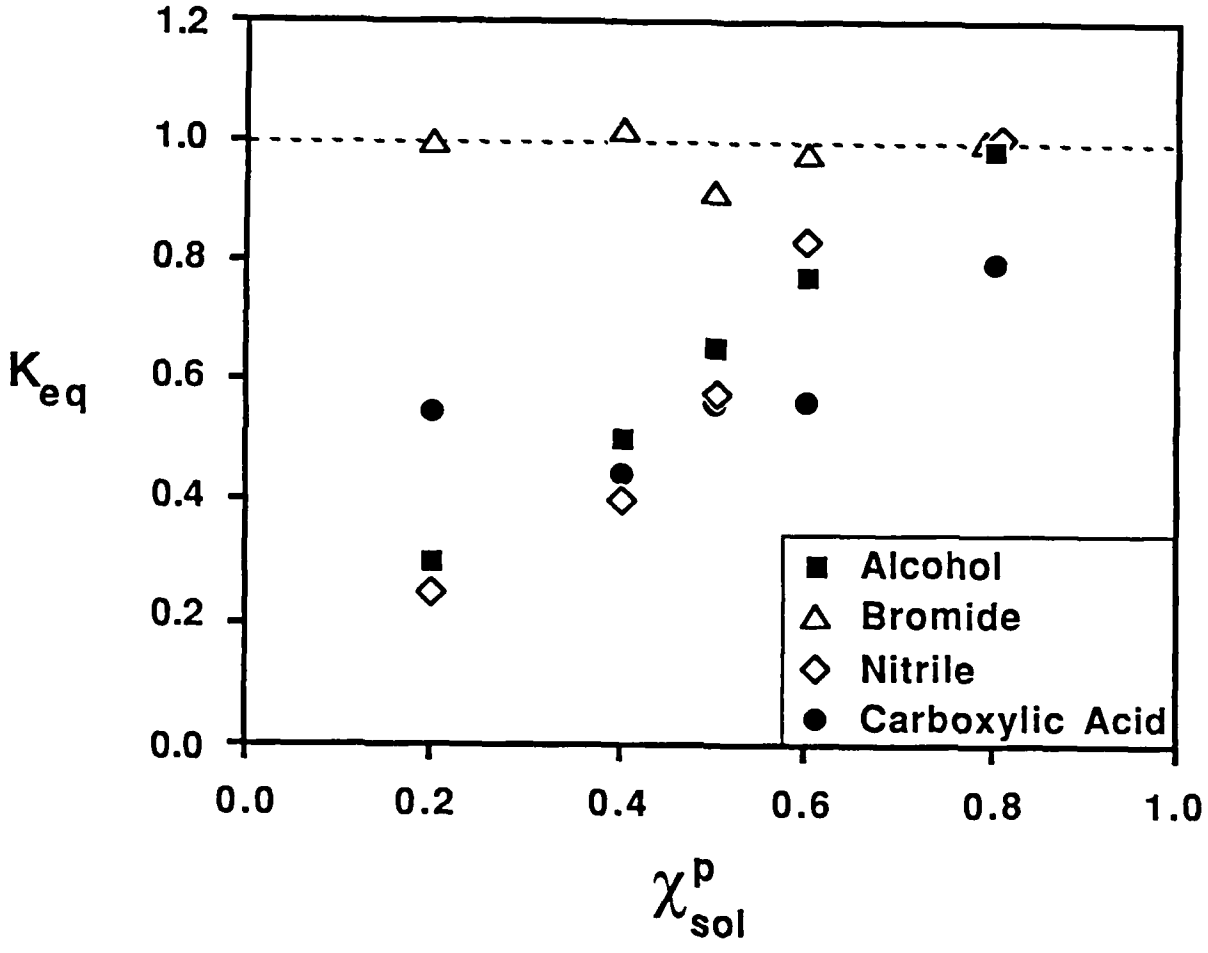

Figure 11. K_{eq} (see text for definition) plotted as a function of the mole fraction of the polar-terminated species in solution for the adsorption of monolayers from solutions in ethanol: $HS(CH_2)_{10}CH_3$ and $HS(CH_2)_{10}CO_2H$ (circles); $HS(CH_2)_8CH_3$ and $HS(CH_2)_8CN$ (diamonds); $HS(CH_2)_{10}CH_3$ and $HS(CH_2)_{10}CH_2Br$ (triangles); and $HS(CH_2)_{10}CH_3$ and $HS(CH_2)_{10}CH_2OH$ (squares). The errors in the values of K_{eq} may be quite large at $\chi^{p}_{sol} = 0.2$ and 0.8, perhaps $\pm$ 0.1.

OH/Me system. Careful study of Fig. 4 reveals that at low concentrations of OH in the surface, the O(1s) photoelectron peak shifted to higher energy by about 0.4 eV. This shift in the peak position implies that the hydroxyl groups are in different environments at low χ^{p}_{surf} and high χ^{p}_{surf}. A possible explanation is that, at low χ^{p}_{surf}, the OH groups in the monolayer are isolated and can only form hydrogen bonds to the solvent . At higher concentrations the OH groups start to aggregate and form H-bonds within the monolayer as well as with the solvent. These interactions would favor monolayers comprising either the pure methyl-terminated species or the pure hydroxyl-terminated species but disfavor monolayers containing a mixture of the two components.[54]

One can postulate a similar rationalization for the data for CN/Me. Poorer solvation of the dipolar nitrile group in the monolayer than in solution would disfavor adsorption of $HS(CH_2)_8CN$. As the concentration of nitrile groups in the monolayer increased, a favorable dipole-dipole interaction could stabilize the nitrile groups at the interface and lead to an increase in K_{eq}.[55]

An unknown factor in these studies is the effect of the structure of the solvent at the monolayer-ethanol interface. As the surface of the monolayer changes from hydrophilic to hydrophobic, the solvent molecules almost certainly reorient to place their methyl groups rather than their alcohol groups adjacent to the monolayer.[56] As a consequence, solvation of polar groups embedded in a largely nonpolar interface might be poor.

The wettability of mixed monolayers is non-ideal. If the two components of a monolayer were to act independently, then the contact angles would follow Cassie's Law,[15]

$$\cos\theta = \chi_1 \cos\theta_1 + \chi_2 \cos\theta_2 \qquad (3)$$

where χ_1 and χ_2 are the mole fractions of the two components in the monolayer and θ_1 and θ_2 are the contact angles on pure monolayers of the two components. Consequently, a

graph of cos θ against χ^{p}_{surf} would be linear (Figure 6). For water on mixed Br/Me surfaces, and for hexadecane on all the surfaces, the intermolecular forces between the monolayer and the probe liquid are largely dispersive and Cassie's Law appears to hold reasonably well (at least over the limited range in which θ_a(HD) is nonzero).[57]

The contact angles of water on surfaces containing alcohol, carboxylic acid, or nitrile groups, in which specific H-bonding interactions are important, deviate strongly from linearity. The apparent hydrophilicity of the polar tail groups is higher when they are in a nonpolar environment composed largely of methyl groups than when their neighbors are other polar groups. Two plausible explanations for these deviations are poor electrostatic solvation of the polar tail groups at low χ^{p} in the low dielectric constant medium provided by the surrounding methyl groups, or poor hydrogen-bonding between dilute protic tail groups in the monolayer. The latter explanation is certainly consistent with the XPS data for the O(1s) photoelectrons and with the form of the adsorption isotherms.

Two-component monolayers do not phase-segregate into macroscopic islands. One of the key questions in this work is the extent to which the two components in the monolayer segregate into discrete islands. A more general problem is to determine the pair correlation function of the components in the monolayer. Alcohols and carboxylic acids self-associate in alkane solvents, so it is likely that association also occurs in the quasi-two-dimensional solution represented by the monolayer. There are several pieces of evidence, however, that suggest that macroscopic islands do not form. In this context we use macroscopic to mean sufficiently large that the properties of the monolayer are determined by molecules of each component that are in an environment indistinguishable from the environment in a pure monolayer of that component.

First, if a monolayer is in equilibrium with a large excess of adsorbate in solution, the chemical potential of the components in solution is independent of the composition of the monolayer. The chemical potential of a molecule in a macroscopic, single-component domain is also essentially independent of the composition of the monolayer. The free

energy of formation of a monolayer composed of macroscopic islands would thus be a linear function of the composition of the monolayer. Consequently, macroscopic, single-component domains would be disfavored thermodynamically with respect to a pure monolayer of the component for which $\mu_{sol} - \mu_{surf}$ is greatest. Islands could form if the composition of the monolayer were kinetically frozen at some non-equilibrium value, with subsequent lateral diffusion resulting in the formation of single-component domains. Although lateral diffusion in the monolayer is *a priori* plausible,[58] evidence such as the preferential adsorption of $HS(CH_2)_{10}CH_2OH$ from solutions in isooctane containing much higher concentrations of $HS(CH_2)_{10}CH_3$ militates against kinetic control over the initial composition of the monolayer.

Second, the contact angles of water on the mixed monolayers do not show the behavior expected of a monolayer composed of discrete islands large enough to influence the contact angle. As discussed earlier, non-polar islands composed of methyl groups would pin the advancing contact angle and cause the plots of cos θ against χ^p_{surf} to be convex rather than concave. Polar islands would pin the receding contact angles and be reflected in greatly increased hysteresis in mixed monolayers, contrary to the relatively constant hysteresis observed on the mixed OH/Me surfaces. It has been estimated theoretically[59] that islands would have to be greater than about 0.1 μm in size to cause observable hysteresis, thus placing an upper bound on the size of any domains, although this limit has not been established experimentally.

Third, a thin film of water condenses onto a pure carboxylic acid surface at 100% relative humidity. Consequently, at 100% RH hexadecane beads on pure monolayers of carboxylic acid-terminated thiols or methyl-terminated thiols (θ_a(HD) = 35–40°. 47° respectively). If the mixed monolayers were to comprise discrete islands, each of which were oleophobic, then the monolayer itself would not be wetted by hexadecane. We observed that hexadecane spread on all the mixed CO_2H/Me monolayers with $\chi^p > 0.4$ at all humidities.

Other evidence suggests that if the two components in the monolayer phase-segregate, the resulting islands must be sufficiently small that the components within each island are still influenced by the other components in the monolayer. First, the non-ideal behavior of the composition and contact angles of the monolayers requires that the energetics of the monolayer vary with composition and hence that the two components in the monolayer interact. Second, the O(1s) peak of the hydroxyl terminus in the XPS spectra of mixed OH/Me monolayers shifts to higher energies and appears to narrow (although the poor signal-to-noise makes accurate widths hard to determine) as the mole fraction of the alcohol in the surface decreases. XPS provides a probe of the local structure in the monolayer: these changes in the shape and position of the O(1s) peak probably arise from interactions with the nearest neighbor molecules in the monolayer and suggest that at low χ^{p}_{surf} aggregates of alcohol groups comprise at most a few molecules. Unfortunately, small changes in peak position and line-widths are not yet understood well enough to draw detailed structural information from XPS. External reflection infrared spectroscopy could distinguish between the presence or absence of hydrogen bonds, but these sub-monolayer densities of hydroxyl groups are near the limit of sensitivity. Third, in another study to be published separately, we have titrated[60] the carboxylic acids in mixed CO_2H/Me surfaces. The onset of ionization shifted to higher pH at lower mole fractions of the acid in the monolayer, suggesting changes in the local environment with composition.

The length of the alkyl chain does not have a major influence on the composition and properties of mixed monolayers containing two thiols of the same chain length. [61] The chain lengths chosen for these studies (n = 8–10) lie between those of long chains (n > 10) for which the properties of the monolayer are largely independent of chain length, and those of short chains (n < 8) in which there are marked changes in the structure and properties with chain length. Fortunately, the results obtained with 11-carbon chains were supported by studies on longer chains: 16-carbon for the CO_2H/Me system,[45] and 19-carbon for OH/Me. The interactions that determine the composition of the

monolayer and its wettability appear to be largely independent of chain length, except perhaps for chains shorter than those studied here.

What is the optimal chain length for studies of mixed monolayers? The eleven-carbon chains, used primarily in these studies, have some advantages over longer chains. Precursor molecules are commercially available with 11 or 16 carbons in the chain. Long-chain molecules, particularly those with more than twenty carbons, become progressively harder to synthesize and purify. Short chains are also more soluble than long chains and allow a wider range of concentration and choice of solvents. Monolayers formed from eleven-carbon chains reach equilibrium, or at least a metastable composition, after immersion overnight in the adsorption solutions: the contact angles of water on the mixed monolayers of $HS(CH_2)_{10}CH_2OH$ and $HS(CH_2)_{10}CH_3$ adsorbed from ethanol did not change upon immersion for an additional ten weeks, and the monolayers adsorbed from acetonitrile were unchanged four months later. On the other hand, the composition of several of the monolayers adsorbed from mixtures of long and short-chain thiols (see companion paper) evolved slowly for several weeks after immersion. Molecules with hydrocarbon chains of sixteen carbons have many of the characteristics that are favorable in both shorter and longer chains. For many studies, sixteen carbons seems to be the optimal chain length.[10,45]

The nature of the solvent has a dramatic effect on the composition of mixed monolayers of $HS(CH_2)_{10}CH_2OH$ and $HS(CH_2)_{10}CH_3$. In ethanol, undecanethiol was adsorbed preferentially from mixtures of $HS(CH_2)_{10}CH_2OH$ and $HS(CH_2)_{10}CH_3$ at all compositions, but particularly at low χ^{p}_{sol}. In acetonitrile, whichever component was more concentrated was adsorbed preferentially. In isooctane, $HS(CH_2)_{10}CH_2OH$ was adsorbed to the almost total exclusion of $HS(CH_2)_{10}CH_3$. This variation in composition with solvent strongly suggests thermodynamic rather than kinetic control over the composition of the monolayer. It is difficult to conceive of a kinetic rationale for the widely different rates of adsorption that would be required for kinetically controlled compositions. It is

well-known that alcohols associate in alkane solutions, largely to form tetramers, but at the low concentrations employed here the monomer predominates.[62] Consequently, the diffusion rates of the two components to the surface should be comparable in an alkane solvent. Furthermore, both tail groups are of similar size and neither is strongly solvated in the alkane solution, so there are no obvious steric grounds for disfavoring one component. The composition of the monolayers can be rationalized qualitatively on thermodynamic grounds by considering the changes in activity of the solutes in different solvents. Long-chain alkanethiols are more soluble in alkane solvents than in ethanol, whereas the converse is true for 11-hydroxyundecanethiol. If one assumes that the activities of the two components in the monolayer are, to first order, independent of the solvent then, as the solvent is made progressively less polar, more of the alcohol-terminated species should be incorporated into the monolayer.

The assumption of thermodynamic equilibrium allows us to rationalize the relationships between the concentrations in solution and the compositions of mixed monolayers of thiols on gold. As we discussed in the introduction, thermodynamic equilibrium requires reversibility of adsorption, or at least some mechanism for interchange of the components in the monolayer and those in solution. Equilibration in fully-formed monolayers (Fig. 1) is clearly not sufficiently rapid to account for the compositions observed after very short immersion times (Figure 10). On the other hand, we are unable to propose a kinetic model that explains the observed data. Thus, although we cannot demonstrate unambiguously that the compositions of the monolayers are under thermodynamic control, the assumption that the compositions of the monolayers are at, or near, their values at thermodynamic equilibrium with the solution provides a framework for interpreting the structure and properties of the mixed monolayers.

The nature of the solvent influences the structure of monolayers of $HS(CH_2)_{10}CH_2OH$. The contact angles of water, ellipsometric thicknesses and XPS data displayed in Table II for monolayers of $HS(CH_2)_{10}CH_3$ and $HS(CH_2)_{10}CH_2OH$ suggest

that the nature of the solvent influences the structure and properties of pure monolayers adsorbed from solution. The inferences that can be drawn from these data are not clear-cut, but several observations are significant.[63] First, the wettability of the monolayers of $HS(CH_2)_{10}CH_3$ did not vary greatly among the adsorption solvents, yet both the ellipsometric thickness and the C/Au ratio from the XPS spectra suggest that the monolayer adsorbed from acetonitrile was significantly thicker than monolayers formed in the other three solvents. Similarly, the monolayers of $HS(CH_2)_{10}CH_2OH$ adsorbed from acetonitrile and ethanol had comparable wettability (both were more hydrophilic than in the previous study shown in Figure 9) but significantly different thicknesses. Changes in the number density of the adsorbed molecules do not appear, on their own, to be sufficient to change the wettability of the monolayers. Second, in ethanol or acetonitrile, the two thiols formed monolayers of approximately the same thickness. The XPS data (and, to a lesser extent, the ellipsometric data) suggest that, in isooctane and hexadecane, the hydroxyl-terminated monolayers were thicker than the methyl-terminated monolayers. The formation of hydrogen bonds between the hydroxyl groups at the surface of the monolayer could alter the packing density of the adsorbed molecules by inducing disorder in the polymethylene backbone or by changing the cant of the chains. In addition, an interfacial structure that optimized intramonolayer H-bonding would minimize the solid-vapor interfacial free energy, γ_{sv}. The interfacial structure adopted in ethanol or acetonitrile, in which the hydroxyl groups can also form H-bonds to the solvent, would result in a higher γ_{sv}. These different values of γ_{sv} could account for the greater wettability of the monolayers of $HS(CH_2)_{10}CH_2OH$ adsorbed from H-bonding solvents.[64] Third, there is no evidence of incorporation of hexadecane into the monolayers: the data obtained from isooctane and hexadecane are very consistent.

The data in Table II suggest strongly that structural differences exist between monolayers adsorbed from different solvents, but the nature of those structural changes is

unclear. Vibrational spectroscopy of these monolayers would be a valuable tool for establishing the structure of these monolayers.

Conclusions

Long-chain alkanethiols formed ordered, oriented monolayers on gold, and were adsorbed preferentially over molecules containing a wide range of other functional groups. None of the other functionalities studied led to monolayers that were clearly superior in quality to those obtained from thiols. Other sulfur-containing species such as disulfides, sulfides, and xanthates also formed monolayers. The only head group that did not contain sulfur and that could be used to form monolayers with contact angles comparable to monolayers of alkanethiols was a trialkylphosphine, R_3P.

Surfaces composed of more than one functional group can be synthesized by coadsorbing thiols with different tail groups from solution. In this paper, we have studied exclusively monolayers containing two components, one of which was terminated by a methyl group. These simple systems are easier to analyze and interpret than more complex monolayers containing additional components or two strongly interacting tail groups. The principles here are generalizable to more complex systems. We make six key observations regarding mixed monolayers:

1) Multi-component monolayers do not segregate into discrete single-component domains. Any islands that do form are too small to influence the contact angle, placing an upper bound of about 0.1 μm on the size of any such islands. The adsorption isotherms and the variation in contact angle with composition and relative humidity suggest further that single-component domains can be no more than a few tens of angstroms across. Changes in acidity and line-shapes in X-ray photoelectron spectra suggest local structural variations on a molecular scale. We have no evidence for two-dimensional order in the tail groups, but the distribution of tail groups is unlikely to be entirely random. The

nonideality of the adsorption isotherms suggests cooperativity between components in the monolayer that would lead to some degree of aggregation .

2) The composition of monolayers adsorbed from solutions containing mixtures of thiols is consistent with thermodynamic control, although equilibrium may not be completely attained in all cases (especially with long alkanethiols) in the intervals studied here (12–24 h). The mechanism for equilibration between the monolayer and solution is unclear: equilibration between a fully-formed monolayer and solution is slow. Equilibration might proceed through a physisorbed thiol prior to transformation to a chemisorbed thiolate. Although the chemisorbed monolayer would not be at equilibrium with the contacting solution, its composition would reflect the equilibrium established in the physisorbed monolayer. Equilibration through a physisorbed thiol plausibly explains the apparent thermodynamic control over the composition, but we have no direct evidence in support of this mechanism, and it is certainly not the only possible mechanism that could account for equilibration between the monolayer and the solution. The composition of the monolayer can be predicted qualitatively by considering the activities of the components in the monolayer and in solution, and specific interactions between the components in the monolayer. The greater the difference in the activities of the two components in solution, the greater will be the preference for adsorption of the component with the higher activity.

3) Mixed monolayers do not act as ideal two-dimensional solutions. In particular, tail groups that form strong hydrogen bonds are disfavored in the nonpolar environment provided by surfaces composed largely of methyl groups. As the proportion of polar groups in the monolayer increases, interactions between tail groups appear to stabilize the polar groups at the interface. In principle, interactions between polar groups could also be unfavorable but were favorable in the three systems studied here.

4) The two components of the monolayer do not act independently in determining the wettability of the surface. Polar groups are more hydrophilic when they are in the

nonpolar environment provided by methyl groups than when the surface of the monolayer is composed largely of other polar group

5) The hysteresis in the contact angle of water on monolayers derived from thiols is small and is approximately independent of the polarity of the tail groups. In mixed monolayers containing a polar and a nonpolar component of the same chain length, the hysteresis is independent of the composition of the monolayer.

6) The nature of the adsorption solvent has a dramatic effect on the composition and wettability of the monolayers. The influence of the solvent on the composition probably occurs largely through changes in the activity of the solutes. The influence on wettability may occur through changes in the structure of the monolayer induced by interactions among tail groups or between tail groups and the solvent. We have no evidence for incorporation of solvent in the monolayers studied here.

Acknowledgements. We are grateful to R. Nuzzo (AT&T Bell Laboratories), to J. Hickman (M.I.T.), and to our colleagues E. B. Troughton, P. Laibinis and H. Biebuyck, who have worked on related systems, for valuable discussions. We thank Prof. A. L. Smith (Unilever) for pointing out the parallels with the behavior of regular solutions.

References and Notes

[1] Supported in part by the ONR and by DARPA. The XPS was provided by DARPA through the University Research Initiative, and is housed in the Harvard University Materials Research Laboratory, an NSF-funded facility.

[2] IBM Pre-Doctoral Fellow in Physical Chemistry 1985-86.

[3] Bigelow, W. C.; Pickett, D. L.; Zisman, W. A. *J. Colloid Sci.* **1946**, *1*, 513-538; Zisman, W. A. In *Contact Angle, Wettability, and Adhesion*; Fowkes, F. M., Ed.; Advances in Chemistry 43; American Chemical Society: Washington, DC, 1964; pp 1–51.

[4] Sagiv, J. *J. Am. Chem. Soc.* **1980**, *102*, 92–98.

[5] Nuzzo, R. G.; Allara, D. L. *J. Am. Chem. Soc.* **1983**, *105*, 4481-4483.

[6] Porter, M. D.; Bright, T. B.; Allara, D. L.; Chidsey, C. E. D. *J. Am. Chem. Soc.* **1987**, *109*, 3559-3568.

[7] Troughton, E. B.; Bain, C. D.; Whitesides, G. M.; Nuzzo, R. G.; Allara, D. L.; Porter, M. D. *Langmuir* **1988**, *4*, 365-385.

[8] Ulman, A.; Tillman, N.; Littman, J., submitted for publication in *J. Phys. Chem.*

[9] Bain, C. D.; Troughton, E. B.; Tao, Y.-T.; Evall, J.; Whitesides, G. M.; Nuzzo, R. G. *J. Am. Chem. Soc.,* in press.

[10] Bain, C. D.; Whitesides, G. M. *J. Am. Chem. Soc.* **1988**, *110*, 5897–5898.

[11] A preliminary communication of this work has been published: Bain, C. D.; Whitesides, G. M. *J. Am. Chem. Soc.* **1988**, *110*, 0000-0000.

[12] Bain, C. D.; Whitesides, G. M. *J. Am. Chem. Soc.* **1988**, *110*, 3665-3666; Bain, C. D.; Whitesides, G. M. *Science (Washington, DC)* **1988**, *240*, 62-63.

[13] Bain, C. D.; Whitesides, G. M. following paper in this issue.

[14] Young's equation relates the solid–liquid, solid–vapor and liquid–vapor interfacial tensions to the contact angle, θ, by $\gamma_{lv} \cos \theta = \gamma_{sv} - \gamma_{sl}$; Young, T. *Phil. Trans. Roy. Soc. (London)* **1805**, *95*, 65–87.

[15] Cassie, A. B. D. *Discuss. Faraday Soc.* **1948**, *3*, 11-16.

[16] Bain, C. D., unpublished results.

[17] Stewart, K. R.; Whitesides, G. M.; Godfried, H. P.; Silvera, I. F. *Rev. Sci. Instrum.* **1986**, *57*, 1381-83.

[18] Chidsey, C. E. D.; Loiacono, D.N.; Sleater, T.; Nakahara, S. *Surf. Sci.* **1988**, *200*, 45-66.

[19] Somorjai, G. A. *Chemistry in Two Dimensions — Surfaces*; Cornell University Press: Ithaca, NY, 1982.

[20] Bain, C. D.; Biebuyck, H. A.; Whitesides, G. M., submitted for publication in *Langmuir*.

[21] Nuzzo, R. G.; Zegarski, B. R.; Dubois, L. H. *J. Am. Chem. Soc.* **1987**, *109*, 733-740.

[22] Displacement of components in the monolayer proceeded relatively rapidly for the first hour, after which the rate of incorporation decreased. The initial rate of exchange also varied with the source of the gold substrates.

[23] Lisowski, E.; Stobinski, L.; Dus, R. *Surf. Sci.* **1987**, *188*, L735-741.

[24] Bigelow, W. C.; Pickett, D. L.; Zisman, W. A. *J. Colloid Sci.* **1946**, *1*, 513-538.

[25] Dettre, R. H.; Johnson, R. E. *J. Phys. Chem.* **1965**, *69*, 1507-1515.

[26] Bain, C. D., unpublished results.

[27] Shirley, D. A. *Phys. Rev. B* **1972**, *5*, 4709-4714.

[28] This procedure for subtraction of the background signal is only approximate. A more accurate approach using peak areas prorated for the number of carbons contributing to the

peak (corrected for the escape depth of the photoelectrons) did not result in appreciably flatter baselines.

[29] Metastable gold oxides can be formed in an oxygen plasma (Ref. 9), electrochemically (Fischer, A. B,; Wrighton, M. S.; Umana, M.; Murray, R. W. *J. Am. Chem. Soc.* **1979**, *101*, 3442–3446) or by direct reaction with oxygen atoms (Ford, R. R.; Pritchard, J. *Chem. Comm.* **1968**, 362-363).

[30] Kostelitz, M.; Domage, J. L.; Oudar, J. *Surf. Sci.* **1973**, *34*, 431-449.

[31] Gao, P.; Weaver, M. J. *J. Phys. Chem.* **1985**, *89*, 5040-5046; Patterson, M. L.; Weaver, M. J. *J. Phys. Chem.* **1985**, *89*, 5046-5051; Chesters, M. A.; Somorjai, G. A. *Surf. Sci.* **1975**, *52*, 21-28.

[32] Finklea, H. O.; Robinson, L. R.; Blackburn, A.; Richter, B.; Allara, D. L.; Bright, T. B. *Langmuir* **1986**, *2*, 238-244; Sabatini, E.; Rubenstein, I.; Maoz, R.; Sagiv, J. *J. Electroanal. Chem.* **1987**, *219*, 365-371.

[33] Gordon, J. G. II; Swalen, J. D. *Opt. Comm.* **1977**, *22*, 374-376.

[34] Laitenen, H. A.; Chao, M. S. *Anal. Chem.* **1961**, *33*, 1836-1838.

[35] For comparison, $[(C_6H_5)_3P]_3Pt$ gives rise to P(2p) signal at 131.4 eV (Riggs, W. M. *Anal. Chem.* **1972**, *44*, 830)

[36] It is likely that some other trivalent phosphorous compounds (such as phosphaalkynes; Kool, L. B., unpublished results) also coordinate to gold.

[37] Wrighton, M.; Ofer, D., personal communication.

[38] Nuzzo, R. G.; Fusco, F. A.; Allara, D. L. *J. Am. Chem. Soc.* **1987**, *109*, 2358-2368.

[39] Li, T. T.-T.; Weaver, M. J. *J. Am. Chem. Soc.* **1984**, *106*, 6107-6108.

[40] Li, T. T.-T.; Liu, H. Y.; Weaver, M. J. *J. Am. Chem. Soc.* **1984**, *106*, 1233-1239.

[41] Surprisingly, octadecyl isothiocyanate and ammonium dodecyldithiocarbamate did not yield high quality monolayers (Laibinis, P., unpublished results).

[42] Rubenstein, I.; Steinberg, S.; Tor, Y.; Shanzer, A.; Sagiv, J. *Nature* **1988**, *332*, 426-429. Monolayers were formed from solutions containing 20 mM octadecanethiol and 20 mM 2,2'-thiobis(ethyl acetoacetate) in 4:1 bicyclohexyl/chloroform. Contact angles of $\theta_a(H_2O) = 108°$, θ_a(bicyclohexyl) = 59° and θ_a(HD) = 57° were reported for these monolayers. The corresponding contact angles on monolayers of octadecanethiol are 112°, 55°, and 47°, respectively (Ref. 9).

[43] On several occasions a small oxygen peak (corresponding to < 5% of the intensity of the peak from a monolayer of $HS(CH_2)_{10}CH_2OH$) was observed on gold slides that had been immersed in the pure methyl-terminated thiol. In these cases the area of this residual oxygen peak was substracted from the areas of all the other samples. The residual oxygen peak was shifted 0.6 eV to lower binding energy from the O(1s) peak arising from the monolayer of $HS(CH_2)_{10}CH_2OH$. Oxygen introduced into the surface by plasma treatment gives rise to a peak shifted a further 1.5 eV to lower energy. The residual oxygen peak is, however, at a similar energy to the photoelectrons observed from silicones, and could arise from trace contamination of the samples by silicone oil.

[44] For clarity, we do not include the solvent in the calculation of the mole fraction in solution. Thus, for two components, A and B, $\chi^{A}_{sol} = [A]_{sol}/([A]_{sol} + [B]_{sol})$.

[45] Holmes-Farley, S. R.; Bain, C. D.; Whitesides, G. M. *Langmuir* **1988**, *4*, 921-937.

[46] Nuzzo, R. G., personal communication.

[47] Levine, O.; Zisman, W. A. *J. Phys. Chem.* **1957**, *61*, 1188-1196; Bewig, K. W.; Zisman, W. A. *J. Phys. Chem.* **1963**, *67*, 130-135; Bartell, L. S.; Betts, J. F. *J. Phys. Chem.* **1960**, *64*, 1075-1076;

[48] During the initial stages of formation of the monolayer, the coverage of the surface and the composition of the monolayer are likely to be determined by the sticking coefficient of

the thiol on the gold surface, and by diffusion of the adsorbates to the gold surface, rather than by interactions between the tail groups of the thiols.

[49] Some other functional groups, such as selenides, that were not studied here, may also form monolayers on gold.

[50] Alkanes interact by dipersive forces; bromoalkanes interact largely by dispersive forces with only a small polar interaction.

[51] Since the polarizability of ethanol and hydrocarbons are similar, differences in the solvation of the methyl group between the solution and the monolayer are probably small.

[52] The term "regular solution" was coined by Hildebrand to refer to solutions with an ideal entropy of mixing but a nonzero enthalpy of mixing (Hildebrand, J. H.; Prausnitz, J. M.; Scott, R. L. *Regular and Related Solutions*; Van Nostrand Reinhold: New York, 1970). By this definition, the mixed monolayers are almost certainly not regular. The sense in which we use regular here is that given by Rowlinson (Rowlinson, J. S. *Liquids and Liquid Mixtures*; Butterworth: London, 1969).

[53] Costas, M.; Patterson, D. J. *Thermochimica Acta*, **1987**, *120*, 161-181.

[54] The mixed monolayers composed of methyl and carboxylic acid-terminated thiols did not exhibit a very low value of K_{eq} at low χ^{P}. A possible explanation is that the carboxylic acids are dimerized at low concentrations in the monolayer. Further spectroscopic studies to determine the nature of the intermolecular interactions at different compositions are needed to resolve questions of aggregation in these monolayers.

[55] The dipole-dipole interaction can be either positive or negative. A favorable interaction implies that the CN moieties in the monolayer are canted at least 35° from the normal to the surface.

[56] The surface tension of ethanol is almost purely dispersive and is comparable in magnitude to alkanes, which suggests that the methyl groups of the ethanol molecule are

oriented outwards at the ethanol–air interface (Harkins, W. D.; Davis, E. C. H.; Clark, G. L. *J. Am. Chem. Soc.* **1917**, *39*, 541–596).

[57] For Cassie's law to hold, the solid-liquid free energy $\gamma_{sl} = \chi_1\gamma_{sl,1} + \chi_2\gamma_{sl,2}$ where $\gamma_{sl,i}$ is the solid-liquid free energy between a pure monolayer of component i and a liquid. Fowkes (Fowkes, F. M.; *Ind. Eng. Chem.* **1964**, *56*(12), 40-52) proposed that for purely dispersive interactions at interfaces the geometric mean approximation can be applied to γ_{sl}. For water on a dispersive solid, Fowkes's approach yields $\gamma_{sl} = \chi_1\gamma_{sv,1} + \chi_2\gamma_{sv,2} + \gamma_{lv} - 2\sqrt{(\gamma^d_{lv}(\chi_1\gamma_{sv,1} + \chi_2\gamma_{sv,2}))}$ where γ^d_{lv} is the dispersive part of the liquid surface free energy. By substituting this expression in Young's equation we obtain cos θ as a function of the surface composition. The geometric mean approximation predicts that cos θ should be convex as a function of χ^p, not linear as predicted by Cassie. The difference between the two predictions for the Br/Me system is small -- less than 3° -- so we cannot make a clear distinction between the two approaches based on our data.

[58] Transmission electron micrographs of thiols on gold (Strong, L.; Whitesides, G. M. *Langmuir* **1988**, *4*, 546-558) suggest that the organic lattice is incommensurate with the underlying gold lattice and hence that the sulfur atoms are not associated with specific sites on the gold surface. Consequently, lateral diffusion on the surface is probably facile in the liquid-like monolayers that exist during the adsorption of the monolayers. In the pseudo-crystalline state of the fully-formed monolayers lateral motion is likely to be much slower, akin to diffusion in organic solids or liquid crystals.

[59] Neumann, A. W.; Good, R. J. *J. Colloid Interface Sci.* **1972**, *38*, 341–358; Schwartz, L. W.; Garoff, S. *Langmuir* **1985**, *1*, 219–230; De Gennes, P. G. *Rev. Mod. Phys.* **1985**, *57*, 828-863.

[60] Holmes-Farley, S. R.; Reamey, R. H.; McCarthy, T. J.; Deutch, J.; Whitesides, G. M. *Langmuir* **1985**, *1*, 725-740.

[61] This statement may not hold for very short chains or for adsorbates with highly dipolar tail groups. Chains with an even number of carbons result in a different orientation of the tail group from chains containing an odd number of carbons (Nuzzo, R. G.; Bain, C. D., unpublished results). Interactions between dipoles are dependent on the orientation of the dipoles, and hence monolayers containing dipolar tail groups may show even-odd variations with chain length.

[62] Costas, M.; Patterson, D. *J. Chem. Soc. Faraday Trans. I* **1985**, *81*, 635-654.

[63] In making inferences based on small differences in contact angles, ellipsometric thicknesses and XPS photoelectron intensities, there is a serious risk of being misled by trace contamination of the surface. We cannot rigorously rule out artifacts due to contamination, however no peaks were observed by XPS from species other than the adsorbed thiolate and the gold substrate.

[64] Ulman (private communication) has obtained a contact angle of 20° for monolayers of hydroxyl-terminated thiols on silver. The hydrocarbon chains in monolayers on silver were less canted than on gold (14° versus 30°) resulting in a different orientation of the hydroxyl groups at the interface with the supernatant water. Clearly the structure, and not merely the number density, of the hydroxyl groups at the monolayer-liquid or monolayer-vapor interface is important in determining wettability.

Figure Captions

Figure 1. Displacement of monolayers of thiols on gold. Advancing contact angle of water as a function of the time of immersion of a preformed monolayer of $HS(CH_2)_{10}CH_3$ in a 1 mM solution of $HS(CH_2)_{10}CH_2OH$ in ethanol (filled circles), and of a preformed monolayer of $HS(CH_2)_{10}CH_2OH$ in a 1 mM solution of $HS(CH_2)_{10}CH_3$ in ethanol (open circles). Note the change in the scale of the abscissa after 100 mins, and the axis break after 900 mins.

Figure 2. Composition of monolayers generated by the coadsorption from ethanol onto gold of $HS(CH_2)_{10}CH_3$ and $[S(CH_2)_{10}CH_2OH]_2$ (squares); and $HS(CH_2)_{10}CH_2OH$ and $[S(CH_2)_{10}CH_3]_2$ (circles). The ordinate represents the ratio of chains in the monolayer derived from the disulfide to those derived from the thiol, as determined by XPS. An estimated error bar (2σ) is shown. If there is a constant preference for adsorption of one species, independent of concentration, the data should fall on straight lines with a slope of one, such as those shown on the graph.

Figure 3. Mole fraction of $HS(CH_2)_{10}CO_2H$ in monolayers adsorbed on gold from mixtures of $HS(CH_2)_{10}CO_2H$ and $HS(CH_2)_{10}CH_3$ in ethanol. The composition of the monolayer was calculated from the intensities of the O(1s) photoelectrons (circles), the ratio of the O(1s) to the $Au(4f_{7/2})$ peaks (triangles), and the intensity of the C(1s) photoelectrons arising from the carboxylic acid group (squares).

Figure 4. O(1s) peak in the XPS spectrum of monolayers adsorbed from mixtures of $HS(CH_2)_{10}CH_2OH$ and $HS(CH_2)_{10}CH_3$ in ethanol. The data were acquired with a pass energy of 100 eV and a spot size of 1 mm. The spectra are shown after subtraction of the background spectrum acquired on the pure $HS(CH_2)_{10}CH_3$ monolayer. The dashed line indicates the peak position for the monolayer of pure $HS(CH_2)_{10}CH_2OH$.

Figure 5. Composition of monolayers adsorbed from ethanolic mixtures of $HS(CH_2)_{10}CH_3$ and $HS(CH_2)_{10}CO_2H$ (circles); $HS(CH_2)_8CH_3$ and $HS(CH_2)_8CN$ (diamonds); $HS(CH_2)_{10}CH_3$ and $HS(CH_2)_{10}CH_2Br$ (triangles); and $HS(CH_2)_{10}CH_3$ and $HS(CH_2)_{10}CH_2OH$ (squares). χ^P represents the mole fraction of the polar-terminated species either in solution or on the surface. The solid and dashed lines are manual fits included simply as a guide to the eye. χ^P_{surf} was calculated from the intensity of the O(1s), N(1s) or Br(3d) photoelectrons. The error bar shown is representative of the random errors (2σ) involved in the analysis of the XPS data.

Figure 6. Advancing contact angles of water (upper figure) and hexadecane (lower figure) on monolayers adsorbed from ethanol onto gold slides: $HS(CH_2)_{10}CH_3$ and $HS(CH_2)_{10}CO_2H$ (circles); $HS(CH_2)_8CH_3$ and $HS(CH_2)_8CN$ (diamonds); $HS(CH_2)_{10}CH_3$ and $HS(CH_2)_{10}CH_2Br$ (triangles); and $HS(CH_2)_{10}CH_3$ and $HS(CH_2)_{10}CH_2OH$ (squares). Errors in contact angles lie within the symbols. A representative error (2σ) bar in χ^P_{surf} is shown. The lines in the upper figure are purely to assist the reader.

Figure 7. Maximum advancing (open circles) and minimum receding contact angles (filled circles) on gold slides after immersion for 2 months in solutions containing mixtures of $HS(CH_2)_{10}CH_3$ and $HS(CH_2)_{10}CH_2OH$.

Figure 8. Comparison of monolayers formed by immersion of gold slides in ethanolic solutions containing mixtures of $HS(CH_2)_{10}CH_3$ and $HS(CH_2)_{10}CH_2OH$ (open symbols), and mixtures of $HS(CH_2)_{18}CH_3$ and $HS(CH_2)_{18}CH_2OH$ (solid symbols) for 12-24 hours: mole fraction of the alcohol-terminated thiol in the monolayer (circles), and advancing contact angles of water (diamonds).

Figure 9. Comparison of monolayers adsorbed onto gold from mixtures of $HS(CH_2)_{10}CH_3$ and $HS(CH_2)_{10}CH_2OH$ dissolved in isooctane (triangles), acetonitrile (circles) and ethanol (squares). Intensity of the O(1s) photoelectron peak normalized to the monolayer adsorbed from a pure solution of $HS(CH_2)_{10}CH_2OH$ (upper figure); advancing contact angle of water (lower figure). The solid (ethanol, isooctane) and dotted lines (acetonitrile) are included simply as guides to the eye.

Figure 10. Advancing contact angle of water as a function of the time of immersion of a gold slide in a 1 mM solution in isooctane containing a 4:1 mixture of $HS(CH_2)_{10}CH_3$ and $HS(CH_2)_{10}CH_2OH$. The open circle represents the contact angle of water on the gold slide before immersion in the solution of the thiols. The first data point shown by a filled circle was obtained by dipping the gold slide in the thiol solution, and immediately removing the slide and rinsing it with clean ethanol.

Figure 11. K_{eq} (see text for definition) plotted as a function of the mole fraction of the polar-terminated species in solution for the adsorption of monolayers from solutions in ethanol: $HS(CH_2)_{10}CH_3$ and $HS(CH_2)_{10}CO_2H$ (circles); $HS(CH_2)_8CH_3$ and $HS(CH_2)_8CN$ (diamonds): $HS(CH_2)_{10}CH_3$ and $HS(CH_2)_{10}CH_2Br$ (triangles); and $HS(CH_2)_{10}CH_3$ and $HS(CH_2)_{10}CH_2OH$ (squares). The errors in the values of K_{eq} may be quite large at $\chi^{P}_{sol} = 0.2$ and 0.8, perhaps $\pm$ 0.1.

DL/1113/89/1

TECHNICAL REPORT DISTRIBUTION LIST, GENERAL

	No. Copies
Office of Naval Research Chemistry Division, Code 1113 800 North Quincy Street Arlington, VA 22217-5000	3
Commanding Officer Naval Weapons Support Center Attn: Dr. Bernard E. Douda Crane, IN 47522-5050	1
Dr. Richard W. Drisko Naval Civil Engineering Laboratory Code L52 Port Hueneme, California 93043	1
Defense Technical Information Center Building 5, Cameron Station Alexandria, Virginia 22314	2 high quality
David Taylor Research Center Dr. Eugene C. Fischer Annapolis, MD 21402-5067	1
Dr. James S. Murday Chemistry Division, Code 6100 Naval Research Laboratory Washington, D.C. 20375-5000	1
Dr. Ronald L. Atkins Chemistry Division (Code 385) Naval Weapons Center China Lake, CA 93555-6001	1
Chief of Naval Research Special Assistant for Marine Corps Matters Code 00MC 800 North Quincy Street Arlington, VA 22217-5000	1
Dr. Bernadette Eichinger Naval Ship Systems Engineering Station Code 053 Philadelphia Naval Base Philadelphia, PA 19112	1
Dr. Sachio Yamamoto Naval Ocean Systems Center Code 52 San Diego, CA 92152-5000	1
David Taylor Research Center Dr. Harold H. Singerman Annapolis, MD 21402-5067 ATTN: Code 283	1

POLYMER PROGRAM DISTRIBUTION LIST

Dr. J. M. Augl
Naval Surface Weapons Center
White Oak, MD 20910

Dr. A. S. Abhiraman
School of Chemical Engineering
Georgia Institute of Technology
Atlanta, GA 30332

4132033

Dr. Harry R. Allcock
Department of Chemistry
Pennsylvania State University
University Park, PA 16802

4132007

Dr. Chris W. Allen
Department of Chemistry
University of Vermont
Burlington, VT 05405

413c012

Dr. Ronald D. Archer
Department of Chemistry
University of Massachusetts
Amherst, MA 01003

413c028

Dr. Ali S. Argon
Mechanical Engineering Department
Massachusetts Institute of Technology
Cambridge, MA 02139

a400005df

Dr. William J. Bailey
Department of Chemistry
University of Maryland
College Park, MD 20742

413a006

Dr. Kurt Baum
Fluorochem, Inc.
680 S. Ayon Avenue
Azusa, CA 91702

4000021sbi

Dr. Frank D. Blum
Department of Chemistry
University of Missouri - Rolla
Rolla, MO 65401

413m005

Dr. Len J. Buckley
Naval Air Development Center
Code 6063
Warminster, PA 18974

Dr. F. James Boerio
Materials Science & Engineering Dept.
University of Cincinnati
Cincinnati, Ohio 45221

413m012

Dr. Ivan Caplan
DTNSRDC Annapolis
Code 0125
Annapolis, MD 21401

Dr. Robert E. Cohen
Department of Chemical Engineering
Massachusetts Institute of Technology
Cambridge, MA 02139

4132001

Dr. E. Fischer
DTNSRDC Code 2853
Annapolis, MD 21402

Dr. Curtis W. Frank
Department of Chemical Engineering
Stanford University
Stanford, CA 94305

413h005

Dr. Gregory S. Girolami
School of Chemical Sciences
University of Illinois
Urbana-Champagne, IL 61801

4132014

Dr. Robert H. Grubbs
Department of Chemistry
California Institute of Technology
Pasadena, CA 91124

4132019

Dr. James F. Haw
Department of Chemistry
Texas A&M University
College Station, TX 77843

413c039

Dr. Stuart L. Cooper
Department of Chemical Engineering
University of Wisconsin
Madison, WI 53706

4132006

Dr. Warren T. Ford
Department of Chemistry
Oklahoma State University
Stillwater, OK 74078

413h006

Dr. John K. Gillham
Department of Chemical Engineering
Princeton University
Princeton, New Jersey 08544

413c005

Dr. Bernard Gordon
Department of Polymer Science
Pennsylvania State University
University Park, PA 16802

413c025

Dr. Henry K. Hall
Department of Chemistry
University of Arizona
Tucson, AZ 85721

413j009

Dr. Alan J. Heeger
Department of Physics
University of California, Santa Barbara
Santa Barbara, CA 93106

4132012

Dr. Pat J. Hendra
Department of Chemistry
University of Southampton
Highfield Southampton 509 5NH
United Kingdom
4134001

Dr. Charles E. Hoyle
Department of Polymer Science
University of Southern Mississippi
Hattiesburg, MS 39406-0076

413c026

Dr. Bruce S. Hudson
Department of Chemistry
University of Oregon
Eugene, Oregon 97403

413c018

Dr. Leonard V. Interrante
Department of Chemistry
Rensselaer Polytechnic Institute
Troy, NY 12181

413c014

Dr. Hatsuo Ishida
Department of Macromolecular Science
Case Western Reserve University
Cleveland, OH 44106

413m008

Dr. Jeffrey T. Koberstein
Institute of Materials Science
University of Connecticut
Storrs, CT 06268

4132013

Dr. Paul M. Lahti
Department of Chemistry
University of Massachusetts
Amherst, MA 01003

413c037

Dr. Richard M. Laine
Washington Technology Center
University of Washington
Seattle, WA 98195

s400033srh

Dr. Robert W. Lenz
Polymer Science and Engineering Dept.
University of Massachusetts
Amherst, MA 01002

441c013

Dr. Geoffrey Lindsay
Chemistry Division - Code 087
Naval Weapons Center
China Lake, CA 93555

4132036

Dr. Alan D. MacDiarmid
Department of Chemistry
University of Pennsylvania
Philadelphia, PA 19104

a400004df

Dr. Chris W. Macosko
Materials Science & Engineering Dept.
University of Minnesota
Minneapolis, MN 55455

4132029

Dr. Joseph H. Magill
Materials Science & Engineering Dept.
University of Pittsburgh
Pittsburgh, PA 15161

413c013

Dr. Leo Mandelkern
Department of Chemistry
Florida State University
Tallahasee, FL 32306-3015

4132018

Dr. Tobin J. Marks
Department of Chemistry
Northwestern University
Evanston, IL 60201

413c030

Dr. Lon J. Mathias
Department of Polymer Science
University of Southern Mississippi
Hattiesburg, MS 30406-0076

413m003

Dr. Krzysztof Matyjaszewski
Department of Chemistry
Carnegie Mellon University
Pittsburgh, PA 15213

413j002

Dr. James E. McGrath
Department of Chemistry
Virginia Polytechnic Institute
Blacksburg, VA 24061

4132007

Dr. William B. Moniz
Code 6120
Naval Research Laboratory
Washington, DC 20375-5000

4132012

Dr. Kay L. Paciorek
Ultrasystems Defense and Space, Inc.
16775 Von Karman Avenue
Irvine, CA 92714

s400029srh

Dr. Virgil Percec
Department of Macromolecular Science
Case Western Reserve University
Cleveland, OH 44106-2699

413c024

Dr. Martin Pomerantz
Department of Chemistry
University of Texas at Arlington
Box 19065
Arlington, TX 76019-0065
a400008df

Dr. Roger S. Porter
Dept. of Polymer Science & Engineering
University of Massachusetts
Amherst, MA 01002

413m006

Dr. T. J. Reinhart, Jr.
Nonmetallic Materials Division
Air Force Materials Laboratory (AFSC)
Wright-Patterson AFB, OH 45433

Dr. Arnost Reiser
Insitute of Imaging Sciences
Polytechnic University
333 Jay Street
Brooklyn, NY 11021

4132022

Dr. Ferdinand Rodriguez
Department of Chemical Engineering
Cornell University
Ithaca, NY 14853

413c011

Dr. Charles M. Roland
Code 6120
Naval Research Laboratory
Washington, DC 20375-5000

413m009

Dr. Michael F. Rubner
Materials Science & Engineering Dept.
Massachusetts Institute of Technology
Cambridge, MA 02139

413m007

Dr. Ronald Salovey
Department of Chemical Engineering
University of Southern California
Los Angeles, CA 90089

413m010

Dr. Jacob Schaefer
Department of Chemistry
Washington University
St. Louis, MO 63130

413m001

Dr. Jerry I. Scheinbeim
Dept. of Mechanics & Materials Science
Rutgers University
Piscataway, NJ 08854

4132009

Dr. Lawrence R. Sita
Department of Chemistry
Carnegie Mellon University
Pittsburgh, PA 15213

4132030

Dr. L. E. Sloter
Code Air 931-A
Naval Air Systems Command
Washington, D. C. 20361-9310

Dr. Richard R. Schrock
Department of Chemistry
Massachusetts Institute of Technology
Cambridge, MA 02139

4132038

Dr. Dietmar Seyferth
Department of Chemistry
Massachusetts Institute of Technology
Cambridge, MA 02139

413c004

Dr. David S. Soane
Department of Chemical Engineering
University of California, Berkeley
Berkeley, CA 94720-9989

413h004

Dr. Les H. Sperling
Materials Research Center #32
Lehigh University
Bethlehem, PA 18015

413c002

Dr. C. S. Sung
Institute of Materials Science
University of Connecticut
Storrs, CT 06268

413m011

Dr. C. H. Wang
Department of Chemistry
University of Utah
Salt Lake City, Utah 84112

413c020

Dr. Robert A. Weiss
Department of Chemical Engineering
University of Connecticut
Storrs, CT 06268

a400006df

Dr. Garth L. Wilkes
Department of Chemical Engineering
Virginia Polytechnic Institute
Blacksburg, VA 24061

4132020

Dr. Richard S. Stein
Polymer Research Institute
University of Massachusetts
Amherst, MA 01002

4132008

Dr. Sukant K. Tripathy
Department of Chemistry
University of Lowell
Lowell, MA 01854

4132016

Dr. Kenneth B. Wagener
Department of Chemistry
University of Florida
Gainesville, FL 32611

a400007df

Dr. George M. Whitesides
Department of Chemistry
Harvard University
Cambridge, MA 02138

4132010